

An overview on deep learning-based approximation methods for partial differential equations

Christian Beck^{1,2}, Martin Hutzenthaler³,
Arnulf Jentzen^{4,5}, Benno Kuckuck⁶

¹ Department of Mathematics, ETH Zurich, Zurich, Switzerland

² Applied Mathematics: Institute for Analysis and Numerics,
Faculty of Mathematics and Computer Science,
University of Münster, Münster, Germany
e-mail: christian.beck@uni-muenster.de

³ Faculty of Mathematics, University of Duisburg-Essen, Essen, Germany
e-mail: martin.hutzenthaler@uni-due.de

⁴ School of Data Science and Shenzhen Research Institute of Big Data,
The Chinese University of Hong Kong, Shenzhen, China
e-mail: ajentzen@cuhk.edu.cn

⁵ Applied Mathematics: Institute for Analysis and Numerics,
Faculty of Mathematics and Computer Science,
University of Münster, Münster, Germany
e-mail: ajentzen@uni-muenster.de

⁶ Applied Mathematics: Institute for Analysis and Numerics,
Faculty of Mathematics and Computer Science,
University of Münster, Münster, Germany
e-mail: bkuckuck@uni-muenster.de

November 21, 2022

Abstract

It is one of the most challenging problems in applied mathematics to approximatively solve high-dimensional partial differential equations (PDEs). Recently, several deep learning-based approximation algorithms for attacking this problem have been proposed and tested numerically on a number of examples of high-dimensional PDEs. This has given rise to a lively field of research in which deep learning-based methods and related Monte Carlo methods are applied to the approximation of high-dimensional PDEs. In this article we offer an introduction to this field of research by revisiting selected mathematical results related to deep learning approximation methods for PDEs and reviewing the main ideas of their proofs. We also provide a short overview of the recent literature in this area of research.

Contents

1	Introduction	2
2	Deep learning-based approximation methods for linear PDEs	3
2.1	Reformulating linear PDEs as infinite dimensional stochastic optimization problems	4
2.2	Mathematical description of deep neural networks (DNNs)	6
2.3	Towards a deep learning-based approximation method for linear PDEs	7

3	Deep learning-based approximation methods for nonlinear PDEs	9
3.1	The deep Galerkin method	9
3.2	The deep splitting approximation method for semilinear PDEs	12
3.3	Other deep learning-based approximation methods for PDEs	15
4	Non-machine learning-based approximation methods for PDEs	18
5	Simulations	19
5.1	Simulations for the deep Galerkin method	19
5.2	Simulations for the deep splitting method	22
6	Theoretical results for DNN approximations for PDEs	24
6.1	Literature overview of theoretical results for DNN approximations for PDEs	24
6.2	Approximation error bounds for DNN approximations for nonlinear heat PDEs . .	25
7	Conclusion	27
8	Source code for simulations	27
8.1	Common source code	27
8.2	Source code for the deep Galerkin method	29
8.3	Source code for the deep splitting method	32

1 Introduction

Partial differential equations (PDEs) are ubiquitous in mathematics as tools for modelling processes in nature or in man-made complex systems. PDEs appear, e.g., as Hamilton–Jacobi–Bellman equations in optimal control problems for describing the value function associated to the control problem, as Zakai or Kushner equations in nonlinear filtering problems for describing the conditional probability distribution of the state of the signal process in the nonlinear filtering problem, in models for the approximative valuation of financial products such as financial derivative contracts, and in the approximative description of the distribution of species in ecosystems to model biodiversity under changing climate conditions. The PDEs which appear in the above-named applications are often nonlinear and high-dimensional where, e.g., in the case of optimal control problems, the PDE dimension $d \in \mathbb{N} = \{1, 2, 3, \dots\}$ corresponds to the number of agents, particles, or resources in the optimal control problem, where, e.g., in the case of the approximative valuation of financial products, the PDE dimension $d \in \mathbb{N}$ corresponds to the number of financial assets (such as stocks, commodities, exchange rates, and interest rates) in the involved hedging portfolio, and where, e.g., in the case of the approximative description of the distribution of species in ecosystems, the PDE dimension $d \in \mathbb{N}$ corresponds to the number of characteristic traits of the species in the ecosystem under consideration.

High-dimensional nonlinear PDEs cannot be solved analytically in nearly all cases and it is one of the most challenging issues in applied mathematics to design and analyze approximation methods for high-dimensional nonlinear PDEs. Standard approximation methods for nonlinear PDEs, such as finite difference approximation methods, finite element approximation methods, spectral Galerkin approximation methods, sparse grid approximation methods, and standard nested Monte Carlo approximation methods, suffer from the so-called curse of dimensionality in the sense that the number of computational operations of the employed approximation scheme grows exponentially in the PDE dimension $d \in \mathbb{N}$ or in the reciprocal $1/\varepsilon$ of the prescribed approximation accuracy $\varepsilon \in (0, \infty)$ and it is a very challenging problem to design and analyze approximation methods for nonlinear PDEs which overcome the curse of dimensionality in the sense that the number of computational operations of the proposed approximation algorithm grows at most polynomially in the PDE dimension $d \in \mathbb{N}$ and in the reciprocal $1/\varepsilon$ of the prescribed approximation accuracy $\varepsilon \in (0, \infty)$.

In the last five years, remarkable progress has been made towards meeting these challenges and deep learning-based approximation methods have proved particularly successful in this regard. Such deep learning-based approximation methods for PDEs have first been proposed in the 1990s

in the case of low-dimensional PDEs, cf., e.g., Dissanayake & Phan-Thien [63], Lagaris et al. [161], and Jianyu et al. [145], and much later, in 2017, in the context of high-dimensional PDEs in E et al. [66], Han et al. [109], Khoo et al. [153], Sirignano & Spiliopoulos [220], Beck et al. [12], E & Yu [70], and Fujii et al. [77]. These methods have since been significantly extended and further studied, and it is one of the goals of this article to provide a rough overview of the recent directions this research has taken.

Beside the challenge of solving PDEs in high dimensions, another area where artificial neural networks seem to provide a powerful tool is in the context of low-dimensional PDEs where not only one fixed solution is desired but instead a whole family of solutions, depending on the initial condition and/or additional parameters, needs to be approximated (parametric PDE approximation problems). Even though the PDE under consideration is low-dimensional, in this context, a high number of parameters leads to a high-dimensional parametric approximation problem, which deep learning approaches seem to be well-suited for; cf., e.g. Khoo et al. [153] and Li et al. [168] and the references mentioned therein.

In this article we intend to introduce the reader to the field of research of deep learning-based approximation of PDEs by revisiting selected results and the main ideas of their proofs as well as providing example implementations in PyTorch and a rough illustration of the capabilities of these methods as applied to some high-dimensional PDE problems. We present two approximation methods for nonlinear PDEs, the so-called deep Galerkin method and the so-called deep splitting method in some detail and we provide a brief outline of the relevant literature in the larger field of deep learning-based approximation methods for PDEs. We note however, that the overview we provide here is by no means comprehensive. A much longer article would be needed to do justice to all the recent developments in this area. Our selection is deliberately biased towards the methods that the authors are most familiar with. While this unfortunately means that many at least equally deserving ideas get rather short shrift, we hope that our introduction encourages the reader to dive deeper into this fast-growing field of research.

The remainder of this article is organized as follows: In Sections 2 and 3 of this article we make the idea of deep learning-based approximation methods more concrete, where we first focus in Section 2 below on selected deep learning-based approximation methods for linear PDEs and, thereafter, we briefly sketch in Sections 3.1 and 3.2 below some key mathematical results connected to selected deep learning-based approximation methods for nonlinear PDEs, as well as providing example implementations. In Section 3.3 we offer a quick overview of the literature on other deep-learning based approximation methods for PDEs. Beside deep learning-based approximation methods, there are also several other approaches in the scientific literature not based on machine learning methods to approximatively solve high-dimensional PDEs. In Section 4 below, we give a short overview of the relevant literature regarding these approaches. In Section 5 below, we present some simulations employing the methods introduced in Section 3, illustrating how these methods can be used to obtain satisfactory results when applied to certain very high-dimensional PDE problems. It should be emphasized that though the literature contains a number of numerical simulations which suggest that deep learning-based approximation methods may have the capacity to overcome the curse of dimensionality in the computation of approximate solutions to high-dimensional PDEs, there are, however, to date only partial theoretical results regarding the conjecture that such methods do indeed overcome the curse of dimensionality. These partial results are briefly reviewed in Section 6 below. An appendix contains the source code used to obtain the simulation results laid out in Section 5.

2 Deep learning-based approximation methods for linear PDEs

In this and the next section of this article (Sections 2 and 3) we briefly outline how some deep learning-based approximation algorithms for PDEs can be derived. In this section we discuss a particular deep learning-based approximation algorithm for linear Kolmogorov PDEs and in Section 3 below we treat two deep learning-based approximation algorithms for nonlinear PDEs, one of which (the deep splitting method discussed in Section 3.2 below) is based on the method presented in this section.

Linear Kolmogorov PDEs can actually be solved approximately without the curse of di-

mensionality by means of standard Monte Carlo approximation methods. However, numerical simulations indicate that deep learning-based approximation algorithms might be more efficient than standard Monte Carlo approximation methods when approximating the solution of a linear Kolmogorov PDE not just at a fixed space-time point but on an entire region such as on high-dimensional cubes (cf., e.g., Beck et al. [11, Section 4]).

In this section we sketch the main ideas of the deep learning-based approximation algorithm for linear Kolmogorov PDEs in [11, Section 3] and our presentation here is strongly inspired by the material in the above-named reference. Roughly speaking, the main idea of the deep learning-based approximation algorithm in [11] is

- (A) to reformulate the linear Kolmogorov PDE whose solution we intend to approximate as a stochastic optimization problem on an infinite dimensional space with the unique solution of the resulting infinite dimensional stochastic optimization problem being the unique solution of the linear Kolmogorov PDE which we intend to approximate,
- (B) to approximate the resulting infinite dimensional stochastic optimization problem through suitable finite dimensional stochastic optimization problems involving deep neural networks (DNNs), and
- (C) to approximately compute the minimizer of the resulting finite dimensional stochastic optimization problems by means of stochastic gradient descent optimization algorithms.

We now make the above procedure more concrete and to further simplify the presentation we restrict ourselves to linear heat PDEs.

2.1 Reformulating linear PDEs as infinite dimensional stochastic optimization problems

In Theorem 2.1 below we, roughly speaking, reformulate linear heat PDEs as stochastic optimization problems on infinite dimensional function spaces (cf. item (A) above). Theorem 2.1 can be proved by an application of the Feynman–Kac formula (cf., e.g., [147, Section 4.4]) and by employing the fact that the expectation of a random variable is the best L^2 -approximation of the random variable (cf., e.g., [11, Lemma 2.1 and Proposition 2.2]). In the scientific literature Theorem 2.1 is, e.g., proved as [11, Corollary 2.4].

Theorem 2.1. *Let $d \in \mathbb{N}$, $T, \rho \in (0, \infty)$, $\varrho = \sqrt{2\rho T}$, $a \in \mathbb{R}$, $b \in (a, \infty)$, let $\varphi: \mathbb{R}^d \rightarrow \mathbb{R}$ be a function, let $u \in C^{1,2}([0, T] \times \mathbb{R}^d, \mathbb{R})$ be a function with at most polynomially growing partial derivatives which satisfies for all $t \in [0, T]$, $x \in \mathbb{R}^d$ that $u(0, x) = \varphi(x)$ and*

$$\frac{\partial u}{\partial t}(t, x) = \rho \Delta_x u(t, x) \quad (1)$$

let $(\Omega, \mathcal{F}, \mathbb{P})$ be a probability space, let $\mathbb{W}: \Omega \rightarrow \mathbb{R}^d$ be a standard normal random variable, let $\xi: \Omega \rightarrow [a, b]^d$ be a continuous uniformly distributed random variable, and assume that \mathbb{W} and ξ are independent. Then

- (i) *there exists a unique $U \in C([a, b]^d, \mathbb{R})$ such that*

$$\mathbb{E}[|\varphi(\varrho \mathbb{W} + \xi) - U(\xi)|^2] = \inf_{v \in C([a, b]^d, \mathbb{R})} \mathbb{E}[|\varphi(\varrho \mathbb{W} + \xi) - v(\xi)|^2], \quad (2)$$

and

- (ii) *it holds for all $x \in [a, b]^d$ that $U(x) = u(T, x)$.*

Roughly speaking, Theorem 2.1 establishes that the solutions of the linear heat PDE in (1) can also be viewed as the solutions of the stochastic optimization problem in (2). The deep learning-based approximation method for linear heat PDEs which we outline within this section is then based on the approach to approximately solve (2) in order to obtain approximations for the solutions of the PDE in (1) (cf. items (A)–(C) above).

While Theorem 2.1 above recasts the solutions of the PDE in (1) at a particular point in time as the solutions of a stochastic optimization problem, we can also derive from this a corollary which shows that the solutions of the PDE over an entire timespan are similarly the solutions of a stochastic optimization problem.

Corollary 2.2. Let $d \in \mathbb{N}$, $T, \rho \in (0, \infty)$, $\varrho = \sqrt{2\rho}$, $a \in \mathbb{R}$, $b \in (a, \infty)$, let $\varphi: \mathbb{R}^d \rightarrow \mathbb{R}$ be a function, let $u \in C^{1,2}([0, T] \times \mathbb{R}^d, \mathbb{R})$ be a function with at most polynomially growing partial derivatives which satisfies for all $t \in [0, T]$, $x \in \mathbb{R}^d$ that $u(0, x) = \varphi(x)$ and

$$\frac{\partial u}{\partial t}(t, x) = \rho \Delta_x u(t, x), \quad (3)$$

let $(\Omega, \mathcal{F}, \mathbb{P})$ be a probability space, let $\mathbb{W}: \Omega \rightarrow \mathbb{R}^d$ be a standard normal random variable, let $\tau: \Omega \rightarrow [0, T]$ be a continuous uniformly distributed random variable, let $\xi: \Omega \rightarrow [a, b]^d$ be a continuous uniformly distributed random variable, and assume that \mathbb{W} , τ , and ξ are independent. Then

(i) there exists a unique $U \in C([0, T] \times [a, b]^d, \mathbb{R})$ which satisfies that

$$\begin{aligned} & \mathbb{E}[|\varphi(\varrho\sqrt{\tau}\mathbb{W} + \xi) - U(\tau, \xi)|^2] \\ &= \inf_{v \in C([0, T] \times [a, b]^d, \mathbb{R})} \mathbb{E}[|\varphi(\varrho\sqrt{\tau}\mathbb{W} + \xi) - v(\tau, \xi)|^2] \end{aligned} \quad (4)$$

and

(ii) it holds for all $t \in [0, T]$, $x \in [a, b]^d$ that $U(t, x) = u(t, x)$.

Proof of Theorem 2.2. Throughout this proof let $F: C([0, T] \times [a, b]^d, \mathbb{R}) \rightarrow [0, \infty]$ satisfy for all $v \in C([0, T] \times [a, b]^d, \mathbb{R})$ that

$$F(v) = \mathbb{E}[|\varphi(\varrho\sqrt{\tau}\mathbb{W} + \xi) - v(\tau, \xi)|^2]. \quad (5)$$

Note that Theorem 2.1 establishes that for all $v \in C([0, T] \times [a, b]^d, \mathbb{R})$, $s \in [0, T]$ it holds that

$$\mathbb{E}[|\varphi(\varrho\sqrt{s}\mathbb{W} + \xi) - v(s, \xi)|^2] \geq \mathbb{E}[|\varphi(\varrho\sqrt{s}\mathbb{W} + \xi) - u(s, \xi)|^2]. \quad (6)$$

Moreover, observe that the assumption that \mathbb{W} , τ , and ξ are independent, the assumption that $\tau: \Omega \rightarrow [0, T]$ is continuous uniformly distributed, and Fubini's theorem ensure that for all $v \in C([0, T] \times [a, b]^d, \mathbb{R})$ it holds that

$$F(v) = \mathbb{E}[|\varphi(\varrho\sqrt{\tau}\mathbb{W} + \xi) - v(\tau, \xi)|^2] = \int_{[0, T]} \mathbb{E}[|\varphi(\varrho\sqrt{s}\mathbb{W} + \xi) - v(s, \xi)|^2] ds. \quad (7)$$

This and (6) prove that for all $v \in C([0, T] \times [a, b]^d, \mathbb{R})$ it holds that

$$F(v) \geq \int_{[0, T]} \mathbb{E}[|\varphi(\varrho\sqrt{s}\mathbb{W} + \xi) - u(s, \xi)|] ds. \quad (8)$$

Combining this with (7) shows that for all $v \in C([0, T] \times [a, b]^d, \mathbb{R})$ it holds that $F(v) \geq F(u)$. Hence we obtain that

$$F(u) = \inf_{v \in C([0, T] \times [a, b]^d, \mathbb{R})} F(v). \quad (9)$$

This and (7) demonstrate that for all $U \in C([0, T] \times [a, b]^d, \mathbb{R})$ with $F(U) = \inf_{v \in C([0, T] \times [a, b]^d, \mathbb{R})} F(v)$ it holds that

$$\int_{[0, T]} \mathbb{E}[|\varphi(\varrho\sqrt{s}\mathbb{W} + \xi) - U(s, \xi)|] ds = \int_{[0, T]} \mathbb{E}[|\varphi(\varrho\sqrt{s}\mathbb{W} + \xi) - u(s, \xi)|] ds. \quad (10)$$

Combining this with (6) proves that for all $U \in C([0, T] \times [a, b]^d, \mathbb{R})$ with $F(U) = \inf_{v \in C([0, T] \times [a, b]^d, \mathbb{R})} F(v)$ there exists $A \subseteq [0, T]$ with $\int_A 1 dx = T$ such that for all $s \in A$ it holds that

$$\mathbb{E}[|\varphi(\varrho\sqrt{s}\mathbb{W} + \xi) - U(s, \xi)|^2] = \mathbb{E}[|\varphi(\varrho\sqrt{s}\mathbb{W} + \xi) - u(s, \xi)|^2]. \quad (11)$$

Theorem 2.1 therefore ensures that for all $U \in C([0, T] \times [a, b]^d, \mathbb{R})$ with $F(U) = \inf_{v \in C([0, T] \times [a, b]^d, \mathbb{R})} F(v)$ there exists $A \subseteq [0, T]$ with $\int_A 1 dx = T$ such that for all $s \in A$ it holds that $U(s) = u(s)$. The fact that $u \in C([0, T] \times [a, b]^d, \mathbb{R})$ hence implies that for all $U \in C([0, T] \times [a, b]^d, \mathbb{R})$ with $F(U) = \inf_{v \in C([0, T] \times [a, b]^d, \mathbb{R})} F(v)$ it holds that $U = u$. Combining this with (9) establishes items (i) and (ii). The proof of Theorem 2.2 is thus complete. \square

2.2 Mathematical description of deep neural networks (DNNs)

In order to be able to give a self-contained presentation of the approximation algorithm sketched in Section 2.1 above, we provide in this subsection a definition of artificial neural networks suitable for stating the results in the following sections. Roughly speaking, a (fully connected feed-forward) artificial neural network is just a description of a function given by alternating compositions of affine linear functions and particular nonlinear functions. More formally, for all $L \in \{2, 3, \dots\}$, $l_0, l_1, \dots, l_L \in \mathbb{N}$, $\Psi_1 \in C(\mathbb{R}^{l_1}, \mathbb{R}^{l_1})$, $\Psi_2 \in C(\mathbb{R}^{l_2}, \mathbb{R}^{l_2})$, \dots , $\Psi_{L-1} \in C(\mathbb{R}^{l_{L-1}}, \mathbb{R}^{l_{L-1}})$ and all affine linear functions $A_1 \in C(\mathbb{R}^{l_0}, \mathbb{R}^{l_1})$, $A_2 \in C(\mathbb{R}^{l_1}, \mathbb{R}^{l_2})$, \dots , $A_L \in C(\mathbb{R}^{l_{L-1}}, \mathbb{R}^{l_L})$ we have that

$$\mathbb{R}^{l_0} \ni x \mapsto (A_L \circ \Psi_{L-1} \circ A_{L-1} \circ \dots \circ \Psi_1 \circ A_1)(x) \in \mathbb{R}^{l_L} \quad (12)$$

is a realization of a (fully connected feed-forward) artificial neural network with architecture (l_0, l_1, \dots, l_L) and activation functions $(\Psi_1, \Psi_2, \dots, \Psi_{L-1})$. The following two concepts, Theorems 2.3 and 2.4 below, make these notions more precise. Theorem 2.3 introduces a notation for affine linear functions. Theorem 2.4 then uses Theorem 2.3 to introduce a notion of artificial neural networks suitable for our purposes.

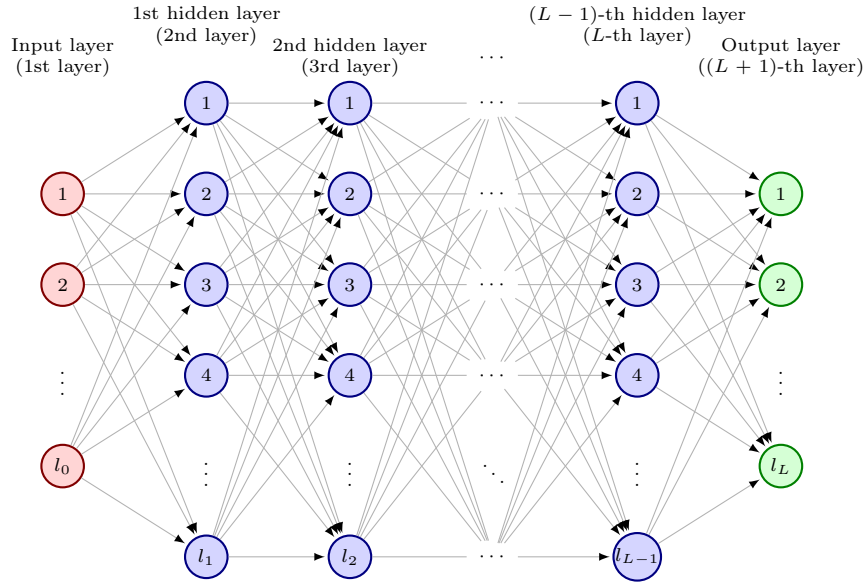


Figure 1: Graphical illustration of a fully-connected feedforward artificial neural network consisting of $L \in \mathbb{N}$ affine linear transformations (i.e., consisting of $L+1$ layers: one input layer, $L-1$ hidden layers, and one output layer) with $l_0 \in \mathbb{N}$ neurons on the input layer, with $l_1 \in \mathbb{N}$ neurons on the first hidden layer, with $l_2 \in \mathbb{N}$ neurons on the second hidden layer, \dots , with l_{L-1} neurons on the $(L-1)$ -th hidden layer, and with l_L neurons in the output layer.

Definition 2.3 (Affine linear functions). Let $\mathfrak{d}, m, n \in \mathbb{N}$, $s \in \mathbb{N}_0$, $\theta = (\theta_1, \theta_2, \dots, \theta_{\mathfrak{d}}) \in \mathbb{R}^{\mathfrak{d}}$ satisfy $\mathfrak{d} \geq s + mn + m$. Then we denote by $\mathcal{A}_{m,n}^{\theta,s} : \mathbb{R}^n \rightarrow \mathbb{R}^m$ the function which satisfies for all $x = (x_1, x_2, \dots, x_n) \in \mathbb{R}^n$ that

$$\mathcal{A}_{m,n}^{\theta,s}(x) = \begin{pmatrix} \theta_{s+1} & \theta_{s+2} & \cdots & \theta_{s+n} \\ \theta_{s+n+1} & \theta_{s+n+2} & \cdots & \theta_{s+2n} \\ \theta_{s+2n+1} & \theta_{s+2n+2} & \cdots & \theta_{s+3n} \\ \vdots & \vdots & \ddots & \vdots \\ \theta_{s+(m-1)n+1} & \theta_{s+(m-1)n+2} & \cdots & \theta_{s+mn} \end{pmatrix} \begin{pmatrix} x_1 \\ x_2 \\ x_3 \\ \vdots \\ x_n \end{pmatrix} + \begin{pmatrix} \theta_{s+mn+1} \\ \theta_{s+mn+2} \\ \theta_{s+mn+3} \\ \vdots \\ \theta_{s+mn+m} \end{pmatrix}. \quad (13)$$

Observe that for all $\mathfrak{d}, m, n \in \mathbb{N}$, $s \in \mathbb{N}_0$, $\theta \in \mathbb{R}^{\mathfrak{d}}$ the definition of $\mathcal{A}_{m,n}^{\theta,s} : \mathbb{R}^n \rightarrow \mathbb{R}^m$ in Theorem 2.3 above refers to the components $\theta_{s+1}, \theta_{s+2}, \dots, \theta_{s+mn+m}$. The condition that $\mathfrak{d} \geq$

$s + mn + m$ hence ensures that the definition of $\mathcal{A}_{m,n}^{\theta,s}: \mathbb{R}^n \rightarrow \mathbb{R}^m$ in (13) above make sense. In Theorem 2.4 below, we now use the affine linear functions introduced in Theorem 2.3 above to define the realizations of artificial neural networks.

Definition 2.4 (Realizations of artificial neural networks). Let $L \in \{2, 3, \dots\}$, $l_0, l_1, \dots, l_L \in \mathbb{N}$, $\Psi_1 \in C(\mathbb{R}^{l_1}, \mathbb{R}^{l_1})$, $\Psi_2 \in C(\mathbb{R}^{l_2}, \mathbb{R}^{l_2})$, \dots , $\Psi_{L-1} \in C(\mathbb{R}^{l_{L-1}}, \mathbb{R}^{l_{L-1}})$ and for every $j \in \{1, 2, \dots, L+1\}$ let $\mathfrak{d}_j \in \mathbb{N}_0$ satisfy $\mathfrak{d}_j = \sum_{k=1}^{j-1} l_k(l_{k-1} + 1)$. Then we denote by $\mathcal{N}_{\Psi_1, \Psi_2, \dots, \Psi_{L-1}}^{l_0, l_1, \dots, l_L}: \mathbb{R}^{\mathfrak{d}_{L+1}} \rightarrow C(\mathbb{R}^{l_0}, \mathbb{R}^{l_L})$ the function which satisfies for all $\theta \in \mathbb{R}^{\mathfrak{d}_{L+1}}$ that

$$(\mathcal{N}_{\Psi_1, \Psi_2, \dots, \Psi_{L-1}}^{l_0, l_1, \dots, l_L})(\theta) = \mathcal{A}_{l_{L-1}, l_L}^{\theta, \mathfrak{d}_L} \circ \Psi_{L-1} \circ \mathcal{A}_{l_{L-2}, l_{L-1}}^{\theta, \mathfrak{d}_{L-1}} \circ \dots \circ \Psi_1 \circ \mathcal{A}_{l_0, l_1}^{\theta, \mathfrak{d}_1} \quad (14)$$

(cf. Theorem 2.3).

We observe that for all $L \in \mathbb{N}$, $l_0, l_1, l_2, \dots, l_L \in \mathbb{N}$, $\Psi_1 \in C(\mathbb{R}^{l_1}, \mathbb{R}^{l_1})$, $\Psi_2 \in C(\mathbb{R}^{l_2}, \mathbb{R}^{l_2})$, \dots , $\Psi_{L-1} \in C(\mathbb{R}^{l_{L-1}}, \mathbb{R}^{l_{L-1}})$ it holds that the image of the function

$$\mathcal{N}_{\Psi_1, \Psi_2, \dots, \Psi_{L-1}}^{l_0, l_1, \dots, l_L}: \mathbb{R}^{\sum_{k=1}^L l_k(l_{k-1} + 1)} \rightarrow C(\mathbb{R}^{l_0}, \mathbb{R}^{l_L}) \quad (15)$$

consists precisely of the realizations of artificial neural networks with architecture (l_0, l_1, \dots, l_L) and activation functions $(\Psi_1, \Psi_2, \dots, \Psi_{L-1})$ as described in (12) above. In this sense the set of (realizations of) artificial neural networks with architecture (l_0, l_1, \dots, l_L) and activation functions $(\Psi_1, \Psi_2, \dots, \Psi_{L-1})$ can be parametrized by real vectors of length $\sum_{k=1}^L l_k(l_{k-1} + 1)$, where the parameter vector comprises the entries of the matrices and vectors used to describe the affine linear maps appearing in the realization function in (14) above. In the case where $L \in \{2, 3, \dots\}$ in Theorem 2.3 satisfies $L \geq 3$ the artificial neural network in (14) above is referred to as a deep neural network. One of the most prominent examples for the activation functions $\Psi_1, \Psi_2, \dots, \Psi_{L-1}$ in (14) is provided by the so-called multidimensional rectifier functions (sometimes also referred to as rectified linear unit (ReLU) functions). These rectifier functions are the subject of the next definition.

Definition 2.5 (Multidimensional rectifier functions). Let $l \in \mathbb{N}$. Then we denote by $\mathbf{r}_l: \mathbb{R}^l \rightarrow \mathbb{R}^l$ the function which satisfies for all $x = (x_1, x_2, \dots, x_l) \in \mathbb{R}^l$ that

$$\mathbf{r}_l(x) = (\max\{x_1, 0\}, \max\{x_2, 0\}, \dots, \max\{x_l, 0\}). \quad (16)$$

In the next subsection, we will employ Theorems 2.4 and 2.5 above to sketch a deep learning-based approximation scheme for linear PDEs.

2.3 Towards a deep learning-based approximation method for linear PDEs

We next explain how the reformulation of a linear PDE as an infinite dimensional stochastic optimization problem from Section 2.1 can be used to derive a deep learning-based approximation method. For this, we now briefly recall the setup from Theorem 2.1. Let $d \in \mathbb{N}$, $T, \rho \in (0, \infty)$, $\varrho = \sqrt{2\rho T}$, $a \in \mathbb{R}$, $b \in (a, \infty)$, let $\varphi: \mathbb{R}^d \rightarrow \mathbb{R}$ be a function, let $u \in C^{1,2}([0, T] \times \mathbb{R}^d, \mathbb{R})$ be a function with at most polynomially growing partial derivatives which satisfies for all $t \in [0, T]$, $x \in \mathbb{R}^d$ that $u(0, x) = \varphi(x)$ and

$$\frac{\partial u}{\partial t}(t, x) = \rho \Delta_x u(t, x), \quad (17)$$

let $(\Omega, \mathcal{F}, \mathbb{P})$ be a probability space, let $\mathbb{W}: \Omega \rightarrow \mathbb{R}^d$ be a standard normal random variable, let $\xi: \Omega \rightarrow [a, b]^d$ be a continuous uniformly distributed random variable, and assume that \mathbb{W} and ξ are independent. Theorem 2.1 then ensures that the solution u of the heat equation in (17) at time T on $[a, b]^d$ is the unique global minimizer of the function

$$C([a, b]^d, \mathbb{R}) \ni v \mapsto \mathbb{E}[\varphi(\varrho \mathbb{W} + \xi) - v(\xi)]^2 \in [0, \infty]. \quad (18)$$

Now an idea of a simple deep learning-based approximation method for PDEs (see [11]) is to approximate the set $C([a, b]^d, \mathbb{R})$ of all continuous functions from $[a, b]^d$ to \mathbb{R} through the set of all

DNNs with a fixed sufficiently large architecture. More formally, let $L \in \{2, 3, \dots\}$, $l_0, l_1, \dots, l_L \in \mathbb{N}$ satisfy $l_0 = d$ and $l_L = 1$ and consider the function

$$\left\{ w \in C([a, b]^d, \mathbb{R}) : \left[\begin{array}{l} \exists \theta \in \mathbb{R}^{\sum_{k=1}^L l_k(l_{k-1}+1)} : \forall x \in [a, b]^d : \\ w(x) = (\mathcal{N}_{\mathbf{r}_{l_1}, \mathbf{r}_{l_2}, \dots, \mathbf{r}_{l_{L-1}}}^{l_0, l_1, \dots, l_L}(\theta))(x) \end{array} \right] \right\} \ni v \quad (19)$$

$$\mapsto \mathbb{E}[|\varphi(\varrho \mathbb{W} + \xi) - v(\xi)|^2] \in [0, \infty]$$

(cf. Theorems 2.4 and 2.5). The approach of the deep learning-based approximation algorithm in [11] is then to approximately compute a suitable minimizer of the function in (19) and to view the resulting approximation of a suitable minimizer of the function in (19) as an approximation of the solution u of the heat equation in (17) at time T on $[a, b]^d$. To approximately compute a suitable minimizer of the function in (19), we reformulate (19) by employing the parametrization function induced by the neural network description in (14) above to obtain the function

$$\mathbb{R}^{\sum_{k=1}^L l_k(l_{k-1}+1)} \ni \theta \mapsto \mathbb{E}[|\varphi(\varrho \mathbb{W} + \xi) - (\mathcal{N}_{\mathbf{r}_{l_1}, \mathbf{r}_{l_2}, \dots, \mathbf{r}_{l_{L-1}}}^{l_0, l_1, \dots, l_L}(\theta))(\xi)|^2] \in [0, \infty]. \quad (20)$$

A suitable minimizer of the function in (20) can then be approximately computed by means of stochastic gradient descent optimization algorithms. The value of the global minimum is typically greater than 0.

A simple implementation of the resulting algorithm in PYTHON using the deep learning framework PyTorch is given in Source Code 1. We refer to [11] for further details on such approximation schemes and we also refer to [11] for numerical simulations for such approximation schemes.

```

1 import torch
2 import math
3
4 # Use the GPU if available
5 dev = torch.device("cuda" if torch.cuda.is_available() else "cpu")
6
7 d = 10          # the input dimension
8 a, b = -3.0, 3.0 # the domain will be [a,b]^d
9 T = 2.0         # the time horizon
10 rho = 1.0       # the diffusivity
11
12 # Define the initial value
13 def phi(x):
14     return torch.cos(x.square().sum(axis=1, keepdim=True))
15
16 # Computes an approximation of E[|phi(sqrt(2*p*T) W + xi) - N(xi)|^2] with W a standard
17 # normal random variable using the rows of x as independent realizations of the
18 # random variable xi
19 def loss(N, rho, phi, T, x):
20     W = torch.randn_like(x).to(dev)
21     return (phi(math.sqrt(2 * rho * T) * W + x) - N(x)).square().mean()
22
23 # Define a neural network with two hidden layers with 50 neurons each using
24 # ReLU activations
25 N = torch.nn.Sequential(
26     torch.nn.Linear(d, 50), torch.nn.ReLU(),
27     torch.nn.Linear(50, 50), torch.nn.ReLU(),
28     torch.nn.Linear(50, 1)
29 ).to(dev)
30
31 # Configure the training parameters and optimization algorithm
32 steps = 1000
33 batch_size = 256
34 optimizer = torch.optim.Adam(N.parameters())
35
36 # Train the network
37 for step in range(steps):
38     # Generate uniformly distributed samples from [a,b]^d
39     x = (torch.rand(batch_size, d) * (b-a) + a).to(dev)

```



```

40 optimizer.zero_grad()
41 # Compute the loss
42 L = loss(N, ρ, φ, T, x)
43 # Compute the gradients
44 L.backward()
45 # Apply changes to weights and biases of N
46 optimizer.step()

```

Source Code 1: A simple implementation in PyTorch of an algorithm based on Theorem 2.1, computing an approximation of the function $[-3, 3]^{10} \ni x \mapsto u(2, x) \in \mathbb{R}$ where $u \in C^{1,2}([0, 2] \times [-3, 3]^{10}, \mathbb{R})$ is the function which satisfies for all $t \in [0, 2]$, $x \in [-3, 3]^{10}$ that $u(0, x) = \cos(\|x\|^2)$ and $\frac{\partial u}{\partial t}(t, x) = \Delta_x u(t, x)$.

In the above outline of a deep learning-based scheme for PDEs we have restricted ourselves to the numerical approximation of the simple heat equation. However, the procedure sketched above also extends to more general linear Kolmogorov PDEs. In particular, the Feynman–Kac formula does not only apply to linear heat PDEs as in (1) above, but can also be applied in the case of linear Kolmogorov PDEs with a possibly nonlinear drift coefficient function $\mu: \mathbb{R}^d \rightarrow \mathbb{R}^d$ and a possibly nonlinear diffusion coefficient function $\sigma: \mathbb{R}^d \rightarrow \mathbb{R}^{d \times d}$. In the PDE the function μ is then multiplied with the first-order partial derivatives of the solution function and the function $\mathbb{R}^d \ni x \mapsto \sigma(x)[\sigma(x)]^* \in \mathbb{R}^{d \times d}$ is multiplied with the Hessian of the solution of the PDE; see, e.g., the PDE in (1.1) in Hairer et al. [106] and Chapter 8.1 in Øksendal [192]. In this case, the Feynman–Kac formula does not involve a simple Brownian motion as in the case of Theorem 2.1 above, but instead involves a stochastic process which cannot be simulated exactly anymore, but which can be approximated by a numerical discretization scheme such as the Euler–Maruyama or the Milstein scheme. We also refer to [11] for further details on this more general case.

3 Deep learning-based approximation methods for nonlinear PDEs

In the previous section we focused on certain deep learning-based approximation methods for linear heat PDEs. We will now turn towards deep learning-based approximation methods for possibly nonlinear PDEs, focusing on two particular such approximation methods and then briefly reviewing the wider literature. More precisely, in Section 3.1 we will provide a derivation of the so-called *deep Galerkin method* (DGM) proposed in Sirignano & Spiliopoulos [220] (see also Dissanayake & Phan-Thien [63] and Lagaris et al. [161] for closely related earlier approaches and Raissi et al. [208] for the method of *physics-informed neural networks* (PINNs), which is also based on the same principle). Then, in Section 3.2, we will give a rough outline of the derivation of the method in [10], which is referred to as the *deep splitting* approximation method. For both the deep Galerkin method and the deep splitting approximation method, we will also provide simple implementations in Python using the PyTorch framework. We will then, in a short and necessarily very incomplete review of the scientific literature in Section 3.3, provide some brief comments on other articles on deep learning-based approximation methods for PDEs.

3.1 The deep Galerkin method

The deep Galerkin method proposed in Sirignano & Spiliopoulos [220] is based on the result in Theorem 3.1 below, which, similar to Theorem 2.1, casts the solution of a certain nonlinear PDE as the solution to a stochastic optimization problem.

For concreteness and simplicity, we state the result here only for semilinear heat PDEs, but we note that the method can easily be adapted to a much wider range of PDEs. We refer, e.g., to Sirignano & Spiliopoulos [220], Raissi et al. [208], the references in Section 3.3, and the much more comprehensive surveys Cuomo et al. [55] and Karniadakis et al. [148] for further information.

Theorem 3.1. Let $T \in (0, \infty)$, $d \in \mathbb{N}$, $g \in C^2(\mathbb{R}^d, \mathbb{R})$, $u \in C^{1,2}([0, T] \times \mathbb{R}^d, \mathbb{R})$, $t \in C([0, T], (0, \infty))$, $x \in C(\mathbb{R}^d, (0, \infty))$, assume that g has at most polynomially growing partial derivatives, let $(\Omega, \mathcal{F}, \mathbb{P})$ be a probability space, let $\mathcal{T}: \Omega \rightarrow [0, T]$ and $\mathcal{X}: \Omega \rightarrow \mathbb{R}^d$ be independent random variables, assume for all $A \in \mathcal{B}([0, T])$, $B \in \mathcal{B}(\mathbb{R}^d)$ that

$$\mathbb{P}(\mathcal{T} \in A) = \int_A t(t) dt \quad \text{and} \quad \mathbb{P}(\mathcal{X} \in B) = \int_B x(x) dx, \quad (21)$$

let $f: \mathbb{R} \rightarrow \mathbb{R}$ be a Lipschitz continuous function, and let $\mathbb{F}: C^{1,2}([0, T] \times \mathbb{R}^d, \mathbb{R}) \rightarrow [0, \infty]$ satisfy for all $v = (v(t, x))_{(t, x) \in [0, T] \times \mathbb{R}^d} \in C^{1,2}([0, T] \times \mathbb{R}^d, \mathbb{R})$ that

$$\mathbb{F}(v) = \mathbb{E}[|v(0, \mathcal{X}) - g(\mathcal{X})|^2 + |\frac{\partial v}{\partial t}(\mathcal{T}, \mathcal{X}) - \Delta_x v(\mathcal{T}, \mathcal{X}) - f(v(\mathcal{T}, \mathcal{X}))|^2]. \quad (22)$$

Then the following two statements are equivalent:

(i) It holds that $\mathbb{F}(u) = \inf_{v \in C^{1,2}([0, T] \times \mathbb{R}^d, \mathbb{R})} \mathbb{F}(v)$.

(ii) It holds for all $t \in [0, T]$, $x \in \mathbb{R}^d$ that $u(0, x) = g(x)$ and

$$\frac{\partial u}{\partial t}(t, x) = \Delta_x u(t, x) + f(u(t, x)). \quad (23)$$

Proof of Theorem 3.1. Observe that (22) implies that for all $v \in C^{1,2}([0, T] \times \mathbb{R}^d, \mathbb{R})$ with $\forall x \in \mathbb{R}^d: u(0, x) = g(x)$ and $\forall t \in [0, T]$, $x \in \mathbb{R}^d: \frac{\partial v}{\partial t}(t, x) = \Delta_x v(t, x) + f(v(t, x))$ it holds that

$$\mathbb{F}(v) = 0. \quad (24)$$

This and the fact that for all $v \in C^{1,2}([0, T] \times \mathbb{R}^d, \mathbb{R})$ it holds that $\mathbb{F}(v) \geq 0$ establish that ((ii) \rightarrow (i)). Note that the assumption that f is a Lipschitz continuous function, the assumption that g is a twice continuously differentiable function, and the assumption that g has at most polynomially growing partial derivatives ensure that there exists $v \in C^{1,2}([0, T] \times \mathbb{R}^d, \mathbb{R})$ which satisfies for all $t \in [0, T]$, $x \in \mathbb{R}^d$ that $v(0, x) = g(x)$ and

$$\frac{\partial v}{\partial t}(t, x) = \Delta_x v(t, x) + f(v(t, x)) \quad (25)$$

(cf., e.g., [15, Corollary 3.4]). This and (24) show that

$$\inf_{v \in C^{1,2}([0, T] \times \mathbb{R}^d, \mathbb{R})} \mathbb{F}(v) = 0. \quad (26)$$

Next observe that (22), (21), and the assumption that \mathcal{T} and \mathcal{X} are independent ensure that for all $v \in C^{1,2}([0, T] \times \mathbb{R}^d, \mathbb{R})$ it holds that

$$\begin{aligned} \mathbb{F}(v) = \int_{[0, T] \times \mathbb{R}^d} & \left(|v(0, x) - g(x)|^2 \right. \\ & \left. + \left| \frac{\partial v}{\partial t}(t, x) - \Delta_x v(t, x) - f(v(t, x)) \right|^2 \right) t(t) x(x) d(t, x). \end{aligned} \quad (27)$$

The assumption that t and x are continuous functions and the fact that for all $t \in [0, T]$, $x \in \mathbb{R}^d$ it holds that $t(t) \geq 0$ and $x(x) \geq 0$ therefore imply that for all $v \in C^{1,2}([0, T] \times \mathbb{R}^d, \mathbb{R})$, $t \in [0, T]$, $x \in \mathbb{R}^d$ with $\mathbb{F}(v) = 0$ it holds that

$$\left(|v(0, x) - g(x)|^2 + \left| \frac{\partial v}{\partial t}(t, x) - \Delta_x v(t, x) - f(v(t, x)) \right|^2 \right) t(t) x(x) = 0. \quad (28)$$

This and the assumption that for all $t \in [0, T]$, $x \in \mathbb{R}^d$ it holds that $t(t) > 0$ and $x(x) > 0$ demonstrate that for all $v \in C^{1,2}([0, T] \times \mathbb{R}^d, \mathbb{R})$, $t \in [0, T]$, $x \in \mathbb{R}^d$ with $\mathbb{F}(v) = 0$ it holds that

$$|v(0, x) - g(x)|^2 + \left| \frac{\partial v}{\partial t}(t, x) - \Delta_x v(t, x) - f(v(t, x)) \right|^2 = 0. \quad (29)$$

Combining this with (26) proves that ((i) \rightarrow (ii)). The proof of Theorem 3.1 is thus complete. \square

Similar to the approach discussed in Section 2.3, the solution to this infinite dimensional stochastic optimization problem can be approximated by the solution to a finite dimensional optimization problem by precomposing the functional in (22) in Theorem 3.1 above with a function parametrizing the set of realizations of artificial neural networks with a fixed sufficiently large architecture and fixed activation functions.

To be more precise, under the assumptions in Theorem 3.1 observe that Theorem 3.1 shows that the solutions of the semilinear heat PDE in (23) are the global minimizers of the function $\mathbb{F}: C^{1,2}([0, T] \times \mathbb{R}^d, \mathbb{R}) \rightarrow [0, \infty]$. In a manner similar to Section 2, a simple deep learning-based approximation method can be derived from this observation by approximating the set $C^{1,2}([0, T] \times \mathbb{R}^d, \mathbb{R})$ through the set of all DNNs with a fixed sufficiently large architecture and fixed activation functions. More formally, let $L \in \{2, 3, \dots\}$, $l_0, l_1, \dots, l_L \in \mathbb{N}$ satisfy $l_0 = d + 1$ and $l_L = 1$, let $\Psi_1 \in C^2(\mathbb{R}^{l_1}, \mathbb{R}^{l_1})$, $\Psi_2 \in C^2(\mathbb{R}^{l_2}, \mathbb{R}^{l_2})$, \dots , $\Psi_{L-1} \in C^2(\mathbb{R}^{l_{L-1}}, \mathbb{R}^{l_{L-1}})$ and consider the function

$$\mathbb{R}^{\sum_{k=1}^L l_k(l_{k-1}+1)} \ni \theta \mapsto \mathbb{F}((\mathcal{N}_{\Psi_1, \Psi_2, \dots, \Psi_{L-1}}^{l_0, l_1, \dots, l_L}(\theta))|_{[0, T] \times \mathbb{R}^d}) \in [0, \infty]. \quad (30)$$

A suitable minimizer of the function in (30) can then be approximately computed using a stochastic gradient descent optimization algorithm (where the derivatives appearing in the definition (22) of the function \mathbb{F} are typically computed using automatic differentiation as supplied by most popular machine learning frameworks) and this minimizer can be considered an approximation of a minimizer of \mathbb{F} and thus an approximation of the solution of the PDE in (23).

An example implementation of the resulting algorithm is given in Source Code 2. For simplicity, we present the algorithm here for a two-dimensional PDE. In Section 5.1 we present numerical simulations using the deep Galerkin method to approximate solutions of certain semi-linear parabolic PDEs in up to 200 dimensions. The source code for these simulations can be found in Section 8.2.

```

1 import torch
2
3 # Use the GPU if available
4 dev = torch.device("cuda" if torch.cuda.is_available() else "cpu")
5
6 # Computes an approximation of  $\mathbb{E}[|v(0, X) - \phi(X)|^2]$  using the rows of  $x$  as independent
7 # realizations of the random variable  $X$ 
8 def dgm_initial_loss(v, phi, x):
9     t = torch.zeros(x.shape[0], 1).to(dev)
10    u = v(torch.cat((t, x), axis=1))
11    return (u - phi(x)).square().mean()
12
13 # Computes an approximation of  $\mathbb{E}[|\partial v / \partial t(T, X) - \Delta_x v(T, X) - f(v(T, X))|^2]$  using the
14 # rows of  $t$  and  $x$  as independent realizations of the random variables  $T$  and  $X$ ,
15 # respectively
16 def dgm_dynamic_loss(v, rho, f, t, x):
17     # Split  $x$  up into components
18     x1, x2 = x[:, 0], x[:, 1]
19     # Compute  $v(t, x)$ 
20     u = v(torch.stack([t, x1, x2], 1))
21     # Compute  $\partial v / \partial t(t, x)$ 
22     u_t = torch.autograd.grad(u, t, torch.ones_like(u), create_graph=True)[0]
23     # Compute  $\Delta_x v(t, x)$ 
24     u_x1 = torch.autograd.grad(u, x1, torch.ones_like(u), create_graph=True)[0]
25     u_x1x1 = torch.autograd.grad(u_x1, x1, torch.ones_like(u_x1),
26                                  create_graph=True)[0]
27     u_x2 = torch.autograd.grad(u, x2, torch.ones_like(u), create_graph=True)[0]
28     u_x2x2 = torch.autograd.grad(u_x2, x2, torch.ones_like(u_x2),
29                                  create_graph=True)[0]
30     Delta_u = u_x1x1 + u_x2x2
31
32     return (u_t - rho * Delta_u - f(u)).square().mean()
33
34 a, b = -3.0, 3.0 # the domain will be  $[a, b]^2$ 
35 T = 2.0         # the time horizon
36 rho = 1.0       # the diffusivity
37

```

```

38 # The initial value of the PDE
39 def  $\varphi(x)$ :
40     return (1. + x.square().sum(axis=1, keepdim=True)).sqrt()
41
42 # The nonlinearity of the PDE
43 def f(y):
44     return torch.sin(y)
45
46 # Define a fully-connected neural network with three hidden layers with
47 # 50 neurons in each hidden layer and using the tanh activation function
48 N = torch.nn.Sequential(
49     torch.nn.Linear(3, 50), torch.nn.Tanh(),
50     torch.nn.Linear(50, 50), torch.nn.Tanh(),
51     torch.nn.Linear(50, 50), torch.nn.Tanh(),
52     torch.nn.Linear(50, 1)
53 ).to(dev)
54
55 # Configure the training parameters and optimization algorithm
56 steps = 250
57 batch_size = 256
58 optimizer = torch.optim.Adam(N.parameters())
59
60 for step in range(steps):
61     # Generate uniformly distributed samples from [0,T]
62     t = T * torch.rand(batch_size).to(dev)
63     t.requires_grad_()
64     # Generate uniformly distributed samples from [a,b]^2
65     x = (torch.rand(batch_size, 2) * (b-a) + a).to(dev)
66     x.requires_grad_()
67
68     optimizer.zero_grad()
69     # Compute the loss
70     loss = dgm_initial_loss(N,  $\varphi$ , x) + dgm_dynamic_loss(N,  $\rho$ , f, t, x)
71     # Compute the gradients
72     loss.backward()
73     # Apply changes to weights and biases of N
74     optimizer.step()

```

Source Code 2: A simple implementation in PyTorch of the deep Galerkin method based on Theorem 3.1, computing an approximation of the function $u \in C^{1,2}([0, 2] \times [-3, 3]^2, \mathbb{R})$ which satisfies for all $t \in [0, 2]$, $x \in [-3, 3]^2$ that $u(0, x) = \sqrt{1 + \|x\|^2}$ and $\frac{\partial u}{\partial t}(t, x) = \Delta_x u(t, x) + \sin(u(t, x))$.

3.2 The deep splitting approximation method for semilinear PDEs

We now focus on the deep splitting approximation method introduced in [10]. The main idea of this method is

- (A) to split up the time interval $[0, T]$, where $T \in (0, \infty)$ is the time horizon of the semilinear PDE under consideration, into the subintervals $[\tau_0, \tau_1], [\tau_1, \tau_2], \dots, [\tau_{N-1}, \tau_N]$ where $N \in \mathbb{N}$, $\tau_0, \tau_1, \dots, \tau_N \in \mathbb{R}$ satisfy $0 = \tau_0 < \tau_1 < \dots < \tau_N = T$, then,
- (B) to freeze the nonlinearity of the semilinear PDE under consideration on each of these subintervals in order to obtain a linear PDE on each of these subintervals, and, thereafter,
- (C) to consecutively apply the deep learning-based approximation method for linear PDEs from Section 2 above to each subinterval.

In this sense the deep splitting approximation method in [10] combines splitting approximations (which are, in the above context, also referred to as exponential Euler approximations; cf., e.g., [51, 103, 122]) with deep learning-based approximations for linear PDEs (see Section 2) to obtain deep learning-based approximations for semilinear PDEs. To formalize this approach, we now present in the following theorem, Theorem 3.2 below, an approximation result which illustrates how a semilinear heat PDE can be approximated through a series of linear heat PDEs (according to item (B) above).

Theorem 3.2. Let $T \in (0, \infty)$, $p \in [1, \infty)$, $f \in C^2(\mathbb{R}, \mathbb{R})$, let $u_d \in C^{1,2}([0, T] \times \mathbb{R}^d, \mathbb{R})$, $d \in \mathbb{N}$, satisfy for all $d \in \mathbb{N}$, $t \in [0, T]$, $x \in \mathbb{R}^d$ that

$$\left(\frac{\partial}{\partial t} u_d\right)(t, x) = (\Delta_x u_d)(t, x) + f(u_d(t, x)), \quad (31)$$

and assume for all $d \in \mathbb{N}$, $i, j \in \{1, 2, \dots, d\}$ that $\sup_{t \in [0, T]} \sup_{x = (x_1, x_2, \dots, x_d) \in \mathbb{R}^d} \left[(1 + \sum_{k=1}^d |x_k|)^{-p} \left(\left| \left(\frac{\partial^2}{\partial x_i \partial x_j} u_d\right)(t, x) \right| + \left| \left(\frac{\partial}{\partial t} u_d\right)(t, x) \right| + |f''(x_1)| + |f'(x_1)| \right) \right] < \infty$. Then

(i) there exist unique at most polynomially growing $\mathcal{U}_n^{d, N} \in C^{1,2}([\frac{(n-1)T}{N}, \frac{nT}{N}] \times \mathbb{R}^d, \mathbb{R})$, $d, N \in \mathbb{N}$, $n \in \{0, 1, \dots, N\}$, which satisfy for all $d, N \in \mathbb{N}$, $n \in \{0, 1, \dots, N-1\}$, $t \in [\frac{nT}{N}, \frac{(n+1)T}{N}]$, $s \in [\frac{-T}{N}, 0]$, $x \in \mathbb{R}^d$ that $\mathcal{U}_{n+1}^{d, N}(\frac{nT}{N}, x) = \mathcal{U}_n^{d, N}(\frac{nT}{N}, x) + \frac{T}{N} f(\mathcal{U}_n^{d, N}(\frac{nT}{N}, x))$, $\mathcal{U}_0^{d, N}(s, x) = u_d(0, x)$, and

$$\left(\frac{\partial}{\partial t} \mathcal{U}_{n+1}^{d, N}\right)(t, x) = (\Delta_x \mathcal{U}_{n+1}^{d, N})(t, x) \quad (32)$$

and

(ii) there exists $c \in \mathbb{R}$ such that for all $d, N \in \mathbb{N}$, $x = (x_1, x_2, \dots, x_d) \in \mathbb{R}^d$ it holds that

$$|\mathcal{U}_N^{d, N}(T, x) - u_d(T, x)| \leq cd^{p+1} N^{-1/2} (1 + \sum_{i=1}^d |x_i|)^p. \quad (33)$$

We now add some comments on the mathematical objects appearing in Theorem 3.2 above. The semilinear heat PDEs in (31) describe the PDEs whose solutions we intend to approximate in Theorem 3.2. The real number $T \in (0, \infty)$ describes the time horizon of the semilinear heat PDEs in (31). The function $f: \mathbb{R} \rightarrow \mathbb{R}$ in Theorem 3.2 specifies the nonlinearity of the semilinear heat PDEs in (31). The functions $u_d: [0, T] \times \mathbb{R}^d \rightarrow \mathbb{R}$, $d \in \mathbb{N}$, in Theorem 3.2 describe the exact solutions of the semilinear heat PDEs in (31).

In Theorem 3.2 we assume that the solutions $u_d: [0, T] \times \mathbb{R}^d \rightarrow \mathbb{R}$, $d \in \mathbb{N}$, of the semilinear heat PDEs in (31) grow at most polynomially. The real number $p \in [1, \infty)$ is used to formulate this polynomial growth assumption in Theorem 3.2. More formally, in Theorem 3.2 it is assumed that for all $d \in \mathbb{N}$ there exists $c \in \mathbb{R}$ such that for all $t \in [0, T]$, $x = (x_1, x_2, \dots, x_d) \in \mathbb{R}^d$ it holds that $|u_d(t, x)| \leq c(1 + \sum_{k=1}^d |x_k|)^p$. In Theorem 3.2 we also assume that $f: \mathbb{R} \rightarrow \mathbb{R}$ is Lipschitz continuous and that the first derivatives of $u_d: [0, T] \times \mathbb{R}^d \rightarrow \mathbb{R}$, $d \in \mathbb{N}$, the second derivatives of $u_d: [0, T] \times \mathbb{R}^d \rightarrow \mathbb{R}$, $d \in \mathbb{N}$, and the second derivative of $f: \mathbb{R} \rightarrow \mathbb{R}$ grow at most polynomially. More specifically, the assumption in Theorem 3.2 that for all $d \in \mathbb{N}$, $i, j \in \{1, 2, \dots, d\}$ it holds that

$$\sup_{t \in [0, T]} \sup_{x = (x_1, x_2, \dots, x_d) \in \mathbb{R}^d} \left[(1 + \sum_{k=1}^d |x_k|)^{-p} \left(|u_d(t, x)| + \left| \left(\frac{\partial}{\partial x_i} u_d\right)(t, x) \right| + \left| \left(\frac{\partial^2}{\partial x_i \partial x_j} u_d\right)(t, x) \right| + \left| \left(\frac{\partial}{\partial t} u_d\right)(t, x) \right| + |f''(x_1)| + |f'(x_1)| \right) \right] < \infty \quad (34)$$

ensures that for all $d \in \mathbb{N}$ there exists $\kappa \in \mathbb{R}$ such that for all $i, j \in \{1, 2, \dots, d\}$, $t \in [0, T]$, $x = (x_1, x_2, \dots, x_d) \in \mathbb{R}^d$, $v, w \in \mathbb{R}$ it holds that $|f(v) - f(w)| \leq \kappa|v - w|$, $|\left(\frac{\partial}{\partial x_i} u_d\right)(t, x)| \leq \kappa(1 + \sum_{k=1}^d |x_k|)^p$, $|\left(\frac{\partial^2}{\partial x_i \partial x_j} u_d\right)(t, x)| \leq \kappa(1 + \sum_{k=1}^d |x_k|)^p$, and $|f''(v)| \leq \kappa(1 + |v|)^p$.

Theorem 3.2 shows that on the subintervals $[0, \frac{T}{N}]$, $[\frac{T}{N}, \frac{2T}{N}]$, \dots , $[\frac{(N-1)T}{N}, T]$ for $N \in \mathbb{N}$ there exist unique at most polynomially growing classical solutions $\mathcal{U}_N^{d, n}: [\frac{(n-1)T}{N}, \frac{nT}{N}] \times \mathbb{R}^d \rightarrow \mathbb{R}$, $d, N \in \mathbb{N}$, $n \in \{1, 2, \dots, N\}$, of the linear heat PDEs in (32) whose initial conditions are specified by means of the initial conditions $\mathbb{R}^d \ni x \mapsto u_d(0, x) \in \mathbb{R}$, $d \in \mathbb{N}$, of the solutions $u_d: [0, T] \times \mathbb{R}^d \rightarrow \mathbb{R}$, $d \in \mathbb{N}$, of the semilinear heat PDEs in (31). Item (ii) in Theorem 3.2 ensures that these unique at most polynomially growing classical solutions $\mathcal{U}_N^{d, n}: [\frac{(n-1)T}{N}, \frac{nT}{N}] \times \mathbb{R}^d \rightarrow \mathbb{R}$, $d, N \in \mathbb{N}$, $n \in \{1, 2, \dots, N\}$, of the linear heat PDEs in (32) can then be used to approximate the solutions $u_d: [0, T] \times \mathbb{R}^d \rightarrow \mathbb{R}$, $d \in \mathbb{N}$, of the semilinear heat PDEs in (31). In particular, observe that item (ii) in Theorem 3.2 proves that for every $d \in \mathbb{N}$, $x \in \mathbb{R}^d$ it holds that the approximation error $|\mathcal{U}_N^{d, N}(T, x) - u_d(T, x)|$ converges to 0 as the number of subintervals N goes to ∞ .

Theorem 3.2 can be proved through applications of the Feynman–Kac formula for linear heat equations (cf., e.g., [106, Corollary 4.17]), the Feynman–Kac formula for semilinear heat

equations (cf., e.g., [15, Theorem 1.1]), and the Gronwall inequality. The proof of Theorem 3.2 is essentially standard, and in order to keep this overview article at a reasonable length we omit here the detailed proof of Theorem 3.2 (cf., e.g., Germain et al. [82, Section 3.2], Cox & van Neerven [51, Section 3], and Jentzen [141, Theorem 2]).

We present in Source Code 3 below a simple implementation of the algorithm sketched in Section 3.2 above based on Theorem 3.2 above. In Section 5.2 we present numerical simulations approximating certain semilinear parabolic PDEs in up to 1000 dimensions. The source code for these simulations can be found in Section 8.3. We refer to [11] for further details on the deep splitting approximation scheme and we also refer to [11] for further numerical simulations for this scheme.

```

1 import torch
2 import math
3
4 # Use the GPU if available
5 dev = torch.device("cuda" if torch.cuda.is_available() else "cpu")
6
7 # Computes an approximation of  $\mathbb{E}[|\varphi(\sqrt{(2\rho T)} W + \xi) - N(\xi)|^2]$  with  $W$  a standard
8 # normal random variable using the rows of  $x$  as independent realizations of the
9 # random variable  $\xi$ 
10 def loss(N,  $\rho$ ,  $\varphi$ , T, x):
11     W = torch.randn_like(x).to(dev)
12     return ( $\varphi(\text{math.sqrt}(2 * \rho * T) * W + x) - N(x)$ ).square().mean()
13
14 d = 10 # the input dimension
15 a, b = -3.0, 3.0 # the domain will be  $[a,b]^d$ 
16 T = 2.0 # the time horizon
17  $\rho$  = 1.0 # the diffusivity
18
19 # The initial value of the PDE
20 def  $\varphi(x)$ :
21     return torch.cos(x.square().sum(axis=1, keepdim=True))
22
23 # The nonlinearity of the PDE
24 def f(y):
25     return torch.sin(y)
26
27 n = 30 # the number of time subintervals
28
29 # Configure the training parameters
30 steps = 1000
31 batch_size = 256
32
33 # Define n neural networks with two hidden layers with 50 neurons each
34 # using ReLU activations
35 N = [
36     torch.nn.Sequential(
37         torch.nn.Linear(d, 50), torch.nn.ReLU(),
38         torch.nn.Linear(50, 50), torch.nn.ReLU(),
39         torch.nn.Linear(50, 1)
40     ).to(dev) for _ in range(n)
41 ]
42
43 for i in range(n):
44     # In this iteration we train the network  $N[i]$ 
45     optimizer = torch.optim.Adam(N[i].parameters())
46
47     # Define the initial value for the linear PDE problem
48     # on the subinterval  $[iT/n, (i+1)T/n]$ 
49     def  $\psi(x)$ :
50         y =  $\varphi(x)$  if  $i==0$  else  $N[i-1](x)$ 
51         return y + T/n * f(y)
52
53     # Train the network
54     for step in range(steps):
55         # Generate uniformly distributed samples from  $[a,b]^d$ 
56         x = (torch.rand(batch_size, d) * (b-a) + a).to(dev)

```

```

57     optimizer.zero_grad()
58     # Compute the loss
59     L = loss(N[i], ρ, ψ, T/n, x)
60     # Compute the gradients
61     L.backward()
62     # Apply changes to weights and biases of N[i]
63     optimizer.step()

```

Source Code 3: A simple implementation in PyTorch of the deep splitting method associated to Theorem 3.2, computing for each $i \in \{1, 2, \dots, 30\}$ an approximation of the function $[-3, 3]^{10} \ni x \mapsto u(\frac{i}{15}, x) \in \mathbb{R}$ where $u \in C^{1,2}([0, 2] \times [-3, 3]^{10}, \mathbb{R})$ is the function which satisfies for all $t \in [0, 2]$, $x \in [-3, 3]^{10}$ that $u(0, x) = \cos(\|x\|^2)$ and $\frac{\partial u}{\partial t}(t, x) = \Delta_x u(t, x) + \sin(u(t, x))$.

3.3 Other deep learning-based approximation methods for PDEs

The methods sketched in Sections 2.3, 3.1, and 3.2 are just three of a large number of machine learning-based approximation schemes for PDEs that have been proposed in the scientific literature. In the following, we provide a short overview of the literature in some strands of research in this area. We make no claims whatsoever to comprehensiveness; in fact, due to the sheer size and rapid development of the field, only a very incomplete view can be attempted here.

Approximation methods for linear PDEs

We refer, e.g., to [11] for approximation methods for linear Kolmogorov PDEs based on discretizations of stochastic differential equations. We refer, e.g., to Sabate Vidales et al. [216] for approximation methods for linear Kolmogorov PDEs based on discretizations of stochastic differential equations in conjunction with suitable control variates. We refer, e.g., to Khoo & Ying [154] for approximation methods for scattering problems associated with linear PDEs of the Helmholtz type based on representing the forward and inverse map by DNNs.

Approximation methods for PDEs based on formulations in terms of backward stochastic differential equations (BSDEs)

The so-called *deep BSDE* method is based on exploiting the equivalence between certain PDEs and BSDEs and approximating the gradient of the solution at discrete time points by DNNs (cf., e.g., Pardoux & Peng [196] for the connection between decoupled BSDEs and semilinear PDEs and cf., e.g., [195, 197] for the connection between coupled BSDEs and quasilinear PDEs). This method was first introduced in E et al. [66] and Han et al. [109] for semilinear parabolic PDEs.

Related approaches for semilinear parabolic PDEs can be found, e.g., in Huré et al. [127] and Chan-Wai-Nam et al. [42], with both these references also containing extensive numerical simulations comparing different approaches. We refer, e.g., to Henry [118] and Pereira et al. [199] for approximation methods for BSDEs building on the deep BSDE approach applied to problems from mathematical finance and robotics, respectively. We refer, e.g., to Han et al. [111] for methods related to the deep BSDE approach suitable for the approximate solution of eigenvalue problems for semilinear second order differential operators; we refer, e.g., to Fujii et al. [77] for refinements of the deep BSDE method suitable for the approximative pricing of American options; we refer, e.g., to Güler et al. [104] for improvements and numerical results for such approximation methods; and we refer, e.g., to Castro [41] for extensions of the method introduced in [127] aimed towards solving non-local nonlinear PDEs. We also refer, e.g., to Nüsken & Richter [191] for approximation methods for Hamilton–Jacobi–Bellman PDEs and control problems based on discretizations of decoupled BSDEs.

The connection between quasilinear parabolic PDEs and coupled BSDEs is exploited, e.g., in Raissi [204] and Han & Long [110] to obtain deep learning-based approximation schemes for quasilinear parabolic PDEs. We refer, e.g., to Ji et al. [143], Andersson et al. [4], and Jiang & Li [144] for further approximation methods for coupled BSDEs. We refer to Gonon et al. [95] for a

study of the approximation methods in [109, 110] when applied to problems of finding risk-sharing equilibria for asset pricing.

In Kremsner et al. [157] the deep BSDE method has been adapted to the approximation of semilinear elliptic PDEs based on time discretizations of BSDEs with random terminal times. Approximation methods based on BSDE representations have also been adapted to fully nonlinear PDEs. We refer, e.g., to Pham et al. [202] and Germain et al. [82] for extensions of the approach in [127] to fully nonlinear PDEs and we refer, e.g., to Beck et al. [12] and Pereira et al. [198] for approximation methods for fully nonlinear PDEs based on extensions of the deep BSDE method employing time discretizations of second order BSDEs. We also refer to Jacquier & Oumgari [136] for approximation methods for certain path-dependent PDEs based on discretizations of BSDEs.

Approximation methods based on least square minimization of the residual

Some of the first attempts at approximatively solving PDEs using artificial neural networks were based on an idea similar to the one presented in Section 3.1 above, i.e., least squares minimization of the residuals of the PDEs under consideration; see, e.g., Dissanayake & Phan-Thien [63] and Lagaris et al. [161] for early articles using this approach. These works use a fixed deterministic set of collocation points and are hence only suitable for low-dimensional PDEs. The *physics-informed neural networks* (PINNs) introduced by Raissi et al. [205, 206] (published as [208]) employ a similar approach but using a fixed set of randomly chosen collocation points throughout training (and integrating observed data into the learning process), see also Berg & Nyström [25] for a similar early example of this approach suitable for complex domains. The DGM variant of the least-squares minimization method presented in Section 3.1 above, based on variable stochastic collocation points was first introduced in Sirignano & Spiliopoulos [220] (see also Carleo & Troyer [38] for a similar method using restricted Boltzmann machines in the approximate solution of Schrödinger PDEs with spins).

Many interesting extensions and variations of the PINN/DGM approach have been proposed in the scientific literature. We refer, e.g., to Anitescu et al. [5] for approximation methods for second order boundary value PDE problems based on adaptive deterministic collocation points, Wang & Perdikaris [225] treats approximation methods for free boundary and Stefan PDE problems. In Yang et al. [235] a PINN approach and generative adversarial networks are combined to obtain approximation methods for stochastic differential equations. We also refer, e.g., to Zhang et al. [239] for approximation methods employing PINNs for low-dimensional nonlinear stochastic PDEs based on generalized Karhunen–Loève type expansions.

The PINN/DGM approach has also been extended to integral equations and non-local PDEs. Some of these methods use classical techniques for the non-local part (see, e.g., Pang et al. [194], Pang et al. [193], Lu et al. [173], and Mishra & Molinaro [186]) and are hence susceptible to the curse of dimensionality, but approaches that are suitable for approximating solutions of high-dimensional PDEs have also been recently investigated (see, e.g., Al-Arabi et al. [3], Deveney et al. [62], Guo et al. [102], and Yuan et al. [237]). We also refer to Haghighat et al. [105] for related attempts at incorporating non-local interactions into a PINN/DGM setting.

There is also a large amount of research focusing on the choice of architectures and methods for improving the training in schemes involving the minimization of the PDE residual; for examples of such works, we refer, e.g., to Meng et al. [183] and Jagtap et al. [137, 140] for methods splitting up the time and/or space domain in order to improve and parallelize training (see also Hu et al. [126] for numerical results and analyses of the generalization error for one such method); we refer, e.g., to Yu et al. [236], McClenny & Braga-Neto [182], Wight & Zhao [233], and Xu et al. [234] for adaptive sampling strategies; we refer, e.g., to Jagtap et al. [138, 139] for training strategies involving activation functions with learnable parameters; we refer, e.g., to Wang et al. [227], Wang et al. [226], and Li et al. [166] for proposals of particular architectures suitable for PINNs; we refer, e.g., to Krishnapriyan et al. [158] and Li et al. [166] for strategies involving weighting of the various terms in the loss function; and we refer, e.g., to Yu et al. [236] for methods involving including the gradient of the residual in the loss function.

For theoretical results giving bounds on the generalization error in the training of DNNs in schemes involving least-squares minimization of the residual of PDEs, we refer, e.g., to Shin et al. [219], Mishra & Molinaro [185], and Hu et al. [126].

Numerous articles in the literature focus on analyzing the performance of the PINN/DGM approach for particular applied problems, see, e.g., Kissas et al. [156], Cai et al. [35], Mao et al. [180], Cai et al. [36], and Jin et al. [146] (though note that these articles treat low-dimensional problems). For further numerical studies of approximation methods for PDEs based on the PINN/DGM approach, we refer, e.g., to Dockhorn [64], Michoski et al. [184], Magill et al. [179], and Gorikhovskii et al. [97].

Though we hope that the above references provide a useful introduction to various directions of research within this area, we note that the PINN/DGM approach has spawned an enormous amount of research activity, which we could not possibly survey in any comprehensive manner here. Cuomo et al. [55] provides a recent overview of this field (see also Karniadakis et al. [148]).

Finally, we refer to Blechschmidt & Ernst [29] for a presentation and comparison of three deep learning-based approaches to approximatively solving PDEs, including one based on least-squares minimization of the residual as well as a BSDE-based approach, notably accompanied by annotated source code in the form of Jupyter notebooks.

Other approximation methods

For extensions of the deep splitting method as presented in Section 3.2 above, we refer to [9] for approximation methods for possibly high-dimensional semilinear stochastic PDEs, and we refer to Boussange et al. [31] and Frey & Köck [75] for approximation methods for non-local PDEs with various boundary conditions.

In E & Yu [70] the so-called *deep Ritz* method, an approximation method for elliptic PDEs based on suitable variational formulations for the PDEs under consideration, is introduced, see also the related methods in, e.g., Khoo et al. [152] and Wang & Zhang [228] and theoretical results in Müller & Zeinhofer [188] and Karumuri et al. [149]. Extensions of such methods suitable for boundary value problems on complex geometries can be found, e.g., in Li et al. [167] and Sheng & Yang [218]. In Samaniego et al. [217] a similar method is applied to problems from computational mechanics. Comparison of methods based on a variational formulation with ones based on least-square minimization of the residual can be found, e.g., in Nabian & Mohammad [189] and Karumuri et al. [149].

Approximation methods based on a Petrov–Galerkin formulation (mostly suitable for low-dimensional PDEs) can be found, e.g., in Kharazmi et al. [150]. Refinements of this method can be found, e.g., in Kharazmi et al. [151], for further numerical results and error analyses we refer, e.g., to Berrone et al. [27, 28].

We refer, e.g., to Han et al. [112] for approximation methods for quasilinear elliptic PDEs based on suitable Feynman–Kac type representations for quasilinear elliptic PDEs. We refer, e.g., to Nakamura-Zimmerer et al. [190] for approximation methods for Hamilton–Jacobi–Bellman PDEs based on Pontryagin’s Minimum Principle and adaptive sampling strategies. We refer, e.g., to Raissi et al. [207] for approximation methods for nonlinear PDEs based on Gaussian process regression.

We refer, e.g., to Zang et al. [238] for approximation methods for nonlinear PDEs based on approximating weak solutions of PDEs using adversarial neural networks.

Particular problems

We refer, e.g., to [8, 18, 19, 48, 98, 127] for approximation methods for American option problems associated with free boundary PDE problems (cf., e.g., [224], [200, Chapter VII], and [192, Section 12.3] for the connection between American options and free boundary PDE problems). We refer, e.g., to [37, 113, 121, 174, 201] for approximation methods for many-electron Schrödinger PDEs. We refer, e.g., to [47, 56, 73, 74, 154, 170, 171, 173, 203, 208, 223, 225, 240] for approximation methods for solving inverse problems associated to PDEs. We refer, e.g., to Han & Hu [107] and Han et al. [108] for approximation methods for Markovian Nash equilibria of stochastic games with a finite number of agents based on approximations for Hamilton–Jacobi–Bellman PDEs and fictitious play. We refer, e.g., to [39, 40, 169, 215] for approximation methods for Markovian Nash equilibria of stochastic games with an infinite number of agents based on mean-field game theory and approximations for Hamilton–Jacobi–Bellman and Fokker–Planck PDEs. We refer, e.g., to Lye et al. [176] for approximation methods for observables of parameterized convection-diffusion

PDEs. We refer, e.g., to [32, 62, 152, 153, 172, 177, 243] for approximation methods for parametric PDE problems based on surrogate modelling.

For further approximation methods for parametric PDEs and corresponding numerical results we refer, e.g., to Geist et al. [81], Li et al. [168] and Becker et al. [20].

Software libraries

For software libraries implementing deep learning-based approximation methods for PDEs, we refer, e.g., to the Python-based libraries DeepXDE (deepxde.readthedocs.io; cf. Lu et al. [173]) and neurodiffEq (pypi.org/project/neurodiffEq; cf. Chen et al. [46]) both implementing the PINN/DGM method and the Julia-based libraries NeuralPDE.jl (neuralpde.sciml.ai; cf. Zubov et al. [244]) implementing the PINN/DGM method as well as the deep BSDE method and HighDimPDE.jl (highdimpde.sciml.ai; cf. Boussange et al. [31]), implementing the deep splitting and full history recursive multilevel Picard (see Section 4 below) methods.

4 Approximation methods for high-dimensional PDEs not based on machine learning

Beside machine learning-based approximation methods for PDEs, there are also several other attempts in the scientific literature to approximately solve high-dimensional nonlinear PDEs. In particular, we refer, e.g., to Darbon & Osher [58] for approximation methods for certain high-dimensional first-order Hamilton–Jacobi–Bellman PDEs. We refer, e.g., to [6, 7, 60, 61, 76, 222, 241, 242] for approximation methods for BSDEs based on spatial grids. We refer, e.g., to [30, 54, 91, 125] for approximation methods for BSDEs based on Malliavin calculus. We refer, e.g., to [22, 88–90, 92, 165, 213, 214] for approximation methods for BSDEs based on suitable projections on function spaces. We refer, e.g., to [44, 52, 53, 59] for approximation methods for BSDEs based on cubature on Wiener space. We refer, e.g., to [43, 162–164] for approximation methods for PDEs based on density estimations and particle systems. We refer, e.g., to [21, 23, 87, 160] for approximation methods based on Picard iterations and suitable projections on function spaces. We refer, e.g., to [34, 78] for approximation methods for BSDEs based on Wiener chaos expansions. We refer, e.g., to [33, 49, 79, 80, 178, 181] for approximation methods for BSDEs based on random walks. We refer, e.g., to [45, 134, 210, 211] for approximation methods for quadratic BSDEs. We refer, e.g., to Abbas-Turki et al. [1, 2] for approximation methods for BSDEs based on nested Monte Carlo approximations. We refer, e.g., to [43, 117, 119, 120, 221, 229, 232] for approximation methods for semilinear parabolic PDEs based on branching diffusion approximations. We refer, e.g., to [65, 71, 124, 212] for approximation methods for BSDEs as well as parabolic and Hamilton–Jacobi–Bellman PDEs based on tensor trains. We refer, e.g., to Warin [230, 231] for approximation methods for semilinear parabolic PDEs based on standard Monte Carlo approximations for nested conditional expectations.

Full history multilevel Picard approximation methods

It should be noted that despite the large amount of research and the great potential that deep-learning based approximation methods for high-dimensional PDEs have shown in numerical simulations, as of today, it has not been rigorously proved that they indeed overcome the curse of dimensionality in the approximation of high-dimensional PDEs. To our knowledge, the only approximation methods for which it has been established in the scientific literature that they overcome the curse of dimensionality in the numerical approximation of semilinear PDEs with general time horizons make up the class of full history recursive multilevel Picard approximation methods (in the following we will abbreviate *full history recursive multilevel Picard* by MLP). MLP approximation methods were introduced in 2016 in E et al. [68, 69] and in 2018 in Hutzenthaler et al. [129] and have been extended and further studied analytically and numerically in [13, 14, 16, 17, 85, 128, 130, 132, 133]. Roughly speaking, MLP approximation methods are based on the idea, first, (I) to reformulate the PDE problem under consideration as a suitable stochastic fixed point equation, then, (II) to approximate the fixed point of the resulting stochastic fixed point equation through fixed point iterates, which in the context of temporal integral

equations are referred to as Picard iterations, and, finally, (III) to approximate the expectations and the integrals appearing in the fixed point iterates through suitable multilevel Monte Carlo approximations. The resulting approximations are full history recursive in the sense that the calculation of the n th MLP iterate employs realizations of the $(n - 1)$ th, $(n - 2)$ th, \dots , 1st MLP iterate. The full history recursive nature of MLP approximation methods is also one of the major differences of MLP approximation methods when compared to standard multilevel Monte Carlo approximations (for references on standard multilevel Monte Carlo approximations see, e.g., [83, 84, 114–116]).

We refer to [69, 85, 129] for MLP approximation methods for semilinear heat PDEs. We refer to [128, 133] for MLP approximation methods for semilinear heat PDEs with gradient-dependent nonlinearities. We refer to [130, 132] for MLP approximation methods for semilinear parabolic PDEs. We refer to [14] for MLP approximation methods for heat PDEs with non-globally Lipschitz continuous nonlinearities. We refer to [13] for MLP approximation methods for semilinear elliptic PDEs. We refer to [16] for MLP approximation methods for nested conditional expectations. We refer to [17, 68] for numerical simulations of MLP approximation methods for semilinear parabolic PDEs. We also refer to the article E et al. [67] for an overview of numerical approximation methods for high-dimensional PDEs.

5 Simulations

In this section we give an illustration of the capabilities of the two approximation methods for nonlinear PDEs presented in Sections 3.1 and 3.2 above by using them to approximate solutions to a sine-Gordon-type PDE of the form

$$\frac{\partial u}{\partial t}(t, x) = \Delta_x u(t, x) + \sin(u(t, x)) \quad (35)$$

for $(t, x) \in (0, T] \times \mathbb{R}^d$ using three different initial values in up to $d = 1000$ dimensions. All the simulations in this section were run on an NVIDIA GEFORCE RTX 3090 GPU with 24 GB of graphics memory, running in a containerized UBUNTU 18.04 instance using 9 cores of an AMD RYZEN THREADRIPPER PRO 3975WX with 37 GB of system memory.

We note that our implementations of both methods are rather naïve, meant to provide easy-to-understand implementations for illustration purposes of these methods, not to obtain state-of-the-art performance. As mentioned in Section 3.3 above, for the deep Galerkin method in particular, a large volume of literature exists regarding DNN architectures and training strategies to improve performance. We also refer to Section 3.3 above for pointers to the literature containing extensive numerical simulations exploring the capabilities of these methods.

We remark that the generally lower accuracy of the deep Galerkin method when compared to the deep splitting method in our simulations is to be expected: While the deep splitting method is tailored to the type of semilinear parabolic PDEs we approximate in this section, the deep Galerkin method uses none of the structure of the PDE problems in question. In fact, this is part of what makes this method so appealing: In principle, it can be applied to nearly any kind of PDE problem and it is often quite trivial to write down a first version of an approximation algorithm, though getting it to converge reliably to a good approximation of the solution can be a significant challenge.

5.1 Simulations for the deep Galerkin method

In this section we present the numerical simulation results of the PDE in (35) in dimensions $d \in \{1, 2, 5, 10, 20, 50, 100, 200\}$ with three different initial values using the deep Galerkin method sketched in Section 3.1 above. For every $d \in \{1, 2, 5, 10, 20, 50, 100, 200\}$ we approximated the solution $u = (u(t, x))_{(t, x) \in [0, 1/2] \times \mathbb{R}^d} \in C([0, 1/2] \times \mathbb{R}^d, \mathbb{R})$ to (35) at time $t = 1/2$ and at $x = 0 \in \mathbb{R}^d$ with the following initial values:

$$\begin{aligned} \mathbb{R}^d \ni x &\mapsto u(0, x) = \sqrt{1 + \|x\|^2} \in \mathbb{R} \\ \mathbb{R}^d \ni x &\mapsto u(0, x) = 2/(4 + \|x\|^2) \in \mathbb{R} \\ \mathbb{R}^d \ni x &\mapsto u(0, x) = \arctan\left(\frac{\|x\|}{2}\right) \in \mathbb{R} \end{aligned} \quad (36)$$

To this end, we trained for every $d \in \{1, 2, 5, 10, 20, 50, 100, 200\}$ a DNN with 3 hidden layers with $d + 1$ neurons in the input layer, $d + 40$ layers in each of the three hidden layers, and 1 neuron in the output layer using the method sketched in Section 3.1. In each of the hidden layers, the affine linear transformation was followed by a multidimensional version of the Mish activation function

$$\mathbb{R} \ni x \mapsto x \tanh(\ln(1 + e^x)) \in \mathbb{R} \quad (37)$$

(cf. Misra [187]). The weights of the affine linear transformations were initialized using Xavier initialization (sometimes also referred to as Glorot initialization) based on a uniform distribution (cf. Glorot & Bengio [86]). For the training, we used the Adam optimization algorithm (cf. Kingma & Ba [155]) with a learning rate decreasing exponentially over the course of the training. More precisely, with an *initial learning rate* $\lambda \in (0, \infty)$ and a *learning rate decay* $\gamma \in (0, 1]$ the learning rate at step k of the training was $\lambda\gamma^k$. The values for the initial learning rate and learning rate decay, as well as the number of training steps were chosen depending on the dimension d and can be found in Tables 1 and 2. For all initial values and all dimensions, we used minibatches of size 256. The collocation points in each training step were sampled from a normal distribution with mean $0 \in \mathbb{R}^d$ and standard deviation depending on the training step. More specifically, in the k -th of n total training steps the collocation points were sampled from a normal distribution with mean $0 \in \mathbb{R}^d$ and covariance $2^{\frac{6(n-k)}{n}-1} I_{\mathbb{R}^d \times d}$.

d	Batch size	Hidden layers	Neurons per hidden layer	Steps	Initial learning rate	Learning rate decay
1	256	3	41	350	0.05	0.98
2	256	3	42	350	0.05	0.98
5	256	3	45	350	0.05	0.98
10	256	3	50	350	0.05	0.98
20	256	3	60	500	0.025	0.99
50	256	3	90	750	0.01	0.995
100	256	3	140	750	0.01	0.995
200	256	3	240	750	0.005	0.995

Table 1: The hyperparameters used in the training for the first and third simulation using the deep Galerkin method (see the results in Tables 3 and 5).

d	Batch size	Hidden layers	Neurons per hidden layer	Steps	Initial learning rate	Learning rate decay
1	256	3	41	500	0.05	0.99
2	256	3	42	500	0.05	0.99
5	256	3	45	500	0.05	0.99
10	256	3	50	750	0.025	0.995
20	256	3	60	750	0.025	0.995
50	256	3	90	1000	0.01	0.998
100	256	3	140	1000	0.01	0.998
200	256	3	240	1000	0.005	0.998

Table 2: The hyperparameters used in the training for the second simulation using the deep Galerkin method (see the results in Table 4).

For each of the three initial values in (36) above and for each $d \in \{1, 2, 5, 10, 20, 50, 100, 200\}$ we ran the deep Galerkin approximation algorithm 20 times independently and recorded the approximation of the solution u of the PDE in (35) with the given initial value at $t = 1/2$ and $x = 0 \in \mathbb{R}^d$. The mean and standard deviation of these values over the 20 independent runs

is given in the second and third columns, respectively, of Tables 3–5 below. The fourth column gives the reference value computed by the MLP method using the code presented in Becker et al. [17]. The fifth column gives an estimation of the absolute L^1 -error of the approximation, computed as the mean over the 20 runs of the distances of the approximation from the reference value. The estimation of the relative L^1 -error in the sixth column is computed as the absolute L^1 -error divided by the absolute value of the reference value. Finally, the average of the runtimes in seconds of the algorithm over the 20 runs is given in the seventh column of Tables 3–5.

d	Mean	Standard deviation	Reference value	Absolute L^1 -error	Relative L^1 -error	Average runtime
1	1.788665	0.013821	1.836708	0.048043	0.026157	2.48
2	2.048171	0.025434	2.109239	0.061302	0.029064	3.47
5	2.684484	0.071031	2.648632	0.057190	0.021592	6.76
10	3.171959	0.027321	3.208623	0.039949	0.012451	17.84
20	4.041396	0.112243	4.107034	0.088848	0.021633	34.38
50	7.193619	0.120224	7.490964	0.297344	0.039694	133.41
100	9.979369	0.409066	9.808476	0.372600	0.037988	292.10
200	13.430278	0.247504	14.604635	1.174357	0.080410	673.06

Table 3: Approximations for $u(1/2, 0, 0, \dots, 0)$ where u is the solution of the PDE in (35) with the initial value $\mathbb{R}^d \ni x \mapsto u(0, x) = \sqrt{1 + \|x\|^2} \in \mathbb{R}$ for $d \in \{1, 2, 5, 10, 20, 50, 100, 200\}$ using the deep Galerkin method. For the hyperparameters used in the training, see Table 1. For the PYTHON source code used to obtain these results, see Section 8.2.

d	Mean	Standard deviation	Reference value	Absolute L^1 -error	Relative L^1 -error	Average runtime
1	0.680122	0.003512	0.677511	0.003552	0.005243	3.62
2	0.590964	0.009817	0.584510	0.010066	0.017221	4.87
5	0.374912	0.033546	0.404080	0.030547	0.075597	9.65
10	0.281780	0.014043	0.258967	0.025007	0.096566	26.19
20	0.139796	0.013930	0.147140	0.013351	0.090739	49.88
50	0.076818	0.005612	0.063228	0.013589	0.214926	175.57
100	0.043529	0.008632	0.032302	0.011817	0.365843	384.41
200	0.020501	0.014760	0.016318	0.012173	0.745950	895.37

Table 4: Approximations for $u(1/2, 0, 0, \dots, 0)$ where u is the solution of the PDE in (35) with the initial value $\mathbb{R}^d \ni x \mapsto u(0, x) = 2/(4 + \|x\|^2) \in \mathbb{R}$ for $d \in \{1, 2, 5, 10, 20, 50, 100, 200\}$ using the deep Galerkin method. For the hyperparameters used in the training, see Table 2. For the PYTHON source code used to obtain these results, see Section 8.2.

d	Mean	Standard deviation	Reference value	Absolute L^1 -error	Relative L^1 -error	Average runtime
1	0.629165	0.029052	0.569925	0.061155	0.107303	2.47
2	0.900790	0.016736	0.835350	0.065440	0.078338	3.52
5	1.249522	0.020660	1.201798	0.047724	0.039711	6.77
10	1.395483	0.022569	1.440293	0.044975	0.031226	18.29
20	1.593871	0.029176	1.622937	0.035450	0.021843	34.28
50	1.789839	0.032926	1.785912	0.027953	0.015652	131.69
100	1.851764	0.034147	1.866269	0.030308	0.016240	291.67
200	1.626139	0.206072	1.921878	0.295739	0.153880	678.89

Table 5: Approximations for $u(1/2, 0, 0, \dots, 0)$ where u is the solution of the PDE in (35) with the initial value $\mathbb{R}^d \ni x \mapsto u(0, x) = \arctan(\frac{\|x\|}{2}) \in \mathbb{R}$ for $d \in \{1, 2, 5, 10, 20, 50, 100, 200\}$ using the deep Galerkin method. For the hyperparameters used in the training of the DNNs, see Table 1. For the PYTHON source code used to obtain these results, see Section 8.2.

5.2 Simulations for the deep splitting method

In this section we present the numerical simulation results for the PDE in (35) in dimensions $d \in \{1, 2, 5, 10, 20, 50, 100, 200, 500, 1000\}$ with three different initial values using the deep splitting method sketched in Section 3.2 above. For every $d \in \{1, 2, 5, 10, 20, 50, 100, 200, 500, 1000\}$ we approximated the solution $u = (u(t, x))_{(t, x) \in [0, 1/2] \times \mathbb{R}^d} \in C([0, 1/2] \times \mathbb{R}^d, \mathbb{R})$ to (35) at time $t = 1/2$ and at $x = 0 \in \mathbb{R}^d$. To this end, we split up the time interval $[0, 1/2]$ into 30 subintervals and successively trained 30 artificial neural networks to approximate the solution u at each of the time points $i/60$ for $i \in \{1, 2, \dots, 30\}$. Each of these artificial neural networks was a fully-connected feedforward neural network with 2 hidden layers with d neurons in the input layer, $d + 50$ neurons in each of the two hidden layers, and 1 neuron in the output layer (except for the one used to approximate the solution at time $T = 1/2$, which consisted of a single affine linear transformation). In each of the hidden layers the affine linear transformation was followed by batch normalization (cf. Ioffe & Szegedy [135]) and a multidimensional version of the exponential linear unit (ELU) activation function

$$\mathbb{R} \ni x \mapsto x + (e^x - 1 - x)\mathbb{1}_{(-\infty, 0]}(x) \in \mathbb{R} \quad (38)$$

(cf. Clevert et al. [50]) The weights of the affine linear transformations were initialized using Xavier initialization based on a uniform distribution (cf. Glorot & Bengio [86]). As for the simulations described in Section 5.1, we used the Adam optimization algorithm with a learning rate decreasing exponentially over the course of the training. The initial learning rate was 0.2 for all simulations. The learning rate decay, as well as the number of training steps were chosen depending on the dimension d and can be found in Tables 1 and 2. For all initial values and all dimensions, we used minibatches of size 256. The sampling of the collocation points used during training was implemented as described in [10]. More specifically, to train the k -th neural network, i.e., the network used to approximate the solution of the PDE in question at time $\frac{kT}{n}$, the collocation points were sampled from a normal distribution with mean $0 \in \mathbb{R}^d$ and covariance $(1 - \frac{k}{30})I_{\mathbb{R}^d \times d}$.

d	Batch size	Hidden layers	Neurons per hidden layer	Steps	Initial learning rate	Learning rate decay
1	256	2	51	350	0.2	0.985
2	256	2	52	350	0.2	0.985
5	256	2	55	350	0.2	0.985
10	256	2	60	350	0.2	0.985
20	256	2	70	500	0.2	0.99
50	256	2	100	500	0.2	0.99
100	256	2	150	750	0.2	0.995
200	256	2	250	1000	0.2	0.995
500	256	2	550	1000	0.2	0.995
1000	256	2	1050	1250	0.2	0.998

Table 6: The hyperparameters used in the training for the simulations using the deep splitting method (see the results in Tables 7–9)

For each of the three initial values in (36) above and for each $d \in \{1, 2, 5, 10, 20, 50, 100, 200, 500, 1000\}$ we ran the deep splitting approximation algorithm 20 times independently and recorded the approximation of the solution u of the PDE in (35) with the given initial value at $t = 1/2$ and $x = 0 \in \mathbb{R}^d$. The columns of the results tables, Tables 7–9 below, follow the same format as in Section 5.1.

d	Mean	Standard deviation	Reference value	Absolute L^1 -error	Relative L^1 -error	Average runtime
1	1.830958	0.015773	1.836708	0.013452	0.007324	20.22
2	2.108470	0.014779	2.109239	0.012182	0.005776	19.90
5	2.642265	0.015791	2.648632	0.014881	0.005618	20.13
10	3.196520	0.016279	3.208623	0.016151	0.005034	20.31
20	4.082424	0.019874	4.107034	0.026197	0.006379	28.89
50	7.480304	0.027910	7.490964	0.022157	0.002958	29.73
100	9.804550	0.009534	9.808476	0.008295	0.000846	46.51
200	14.602816	0.036716	14.604635	0.020845	0.001427	64.86
500	21.386109	1.045499	22.230142	0.844033	0.037968	75.23
1000	31.748045	0.126012	31.751259	0.068201	0.002148	117.77

Table 7: Approximations for $u(1/2, 0, 0, \dots, 0)$ where u is the solution of the PDE in (35) with the initial value $\mathbb{R}^d \ni x \mapsto u(0, x) = \sqrt{1 + \|x\|^2} \in \mathbb{R}$ for $d \in \{1, 2, 5, 10, 20, 50, 100, 200, 500, 1000\}$ using the deep splitting method. For the hyperparameters used in the training of the DNNs, see Table 6. For the PYTHON source code used to obtain these results, see Section 8.3.

d	Mean	Standard deviation	Reference value	Absolute L^1 -error	Relative L^1 -error	Average runtime
1	0.678383	0.004441	0.677511	0.003652	0.005390	20.24
2	0.583808	0.005164	0.584510	0.004229	0.007235	19.93
5	0.405637	0.003722	0.404080	0.003680	0.009107	20.08
10	0.257737	0.001830	0.258967	0.001949	0.007524	20.33
20	0.146415	0.000674	0.147140	0.000859	0.005841	29.08
50	0.062905	0.000134	0.063228	0.000323	0.005114	30.05
100	0.032181	0.000150	0.032302	0.000146	0.004514	46.48
200	0.016254	0.000023	0.016318	0.000064	0.003941	64.93
500	0.006542	0.000005	0.006568	0.000026	0.003909	75.37
1000	0.003277	0.000010	0.003291	0.000015	0.004467	118.31

Table 8: Approximations for $u(1/2, 0, 0, \dots, 0)$ where u is the solution of the PDE in (35) with the initial value $\mathbb{R}^d \ni x \mapsto u(0, x) = 2/(4 + \|x\|^2) \in \mathbb{R}$ for $d \in \{1, 2, 5, 10, 20, 50, 100, 200, 500, 1000\}$ using the deep splitting method. For the hyperparameters used in the training of the DNNs, see Table 6. For the PYTHON source code used to obtain these results, see Section 8.3.

d	Mean	Standard deviation	Reference value	Absolute L^1 -error	Relative L^1 -error	Average runtime
1	0.561503	0.012954	0.569925	0.012631	0.022162	20.16
2	0.830821	0.011572	0.835350	0.009811	0.011745	20.19
5	1.195350	0.007251	1.201798	0.008002	0.006658	20.09
10	1.436600	0.003500	1.440293	0.004196	0.002913	20.22
20	1.622351	0.001493	1.622937	0.001305	0.000804	29.17
50	1.785940	0.000271	1.785912	0.000214	0.000120	29.81
100	1.866438	0.000438	1.866269	0.000337	0.000181	46.65
200	1.922286	0.000091	1.921878	0.000408	0.000212	65.01
500	1.970859	0.000031	1.970294	0.000566	0.000287	75.16
1000	1.994976	0.000086	1.994330	0.000645	0.000324	118.21

Table 9: Approximations for $u(1/2, 0, 0, \dots, 0)$ where u is the solution of the PDE in (35) with the initial value $\mathbb{R}^d \ni x \mapsto u(0, x) = \arctan(\frac{\|x\|}{2}) \in \mathbb{R}$ for $d \in \{1, 2, 5, 10, 20, 50, 100, 200, 500, 1000\}$ using the deep splitting method. For the hyperparameters used in the training of the DNNs, see Table 6. For the PYTHON source code used to obtain these results, see Section 8.3.

6 Theoretical results for DNN approximations for PDEs

In this section we will briefly mention some of the results that exist in the scientific literature which attempt to explain in theoretical terms the success of deep learning-based approximation methods for high-dimensional PDEs in numerical simulations. We first provide a general introduction to the topic (see Section 6.1) and then review the main result in Hutzenthaler et al. [131] as one instance of a mathematical result providing a partial error bound for deep learning-based approximation methods for PDEs (see Section 6.2).

6.1 Literature overview of theoretical results for DNN approximations for high-dimensional PDEs

Although by now a large number of highly encouraging numerical simulations hinting at the great potential of deep learning-based methods in the approximation of high-dimensional PDEs can be found in the scientific literature (see the references in Section 3.3; cf. Section 5 above), there is as yet no mathematical result rigorously explaining the great practical success of deep learning-based approximation methods for PDEs. In particular, so far there does not exist a proof that deep learning-based methods are capable of overcoming the curse of dimensionality in the approximative computation of solutions of high-dimensional PDEs in the sense that the number of computational operations necessary for calculating the numerical approximation of the PDE under consideration grows at most polynomially in the PDE dimension $d \in \mathbb{N}$ and the reciprocal $1/\varepsilon$ of the prescribed approximation accuracy $\varepsilon \in (0, \infty)$.

However, recent results supplying rigorous partial error analyses show that DNNs at least possess the necessary expressive power to overcome the curse of dimensionality in the approximation of high-dimensional PDEs in the sense that there exist DNN approximations for high-dimensional PDEs with the number of parameters used to describe the approximating neural network growing at most polynomially in the PDE dimension $d \in \mathbb{N}$ and the reciprocal $1/\varepsilon$ of

the prescribed approximation accuracy $\varepsilon \in (0, \infty)$. The first result in this direction was obtained in 2018 in Grohs et al. [100] and, since then, a number of articles have appeared significantly extending the results in Grohs et al. [100], covering several more classes of PDEs (see, e.g., [24, 26, 72, 94, 96, 99, 101, 123, 131, 142, 159, 209]). In particular, in [131] there is now also a result on nonlinear PDEs in the scientific literature which shows that DNNs have the expressive power to overcome the curse of dimensionality in the numerical approximation of solutions of nonlinear heat PDEs with Lipschitz continuous nonlinearities.

To give the reader a somewhat more complete picture on theoretical results for DNN approximations for PDEs, we also refer, e.g., to Han & Long [110] and Huré et al. [127] for conditional convergence rate results for approximation errors for deep learning-based approximations for PDEs, we also refer, e.g., to Luo & Yang [175], Shin et al. [219], Mishra & Molinaro [185], and Hu et al. [126] for upper bounds for the generalization error for deep learning-based approximations for PDEs, we also refer, e.g., to Darbon et al. [56] and Darbon & Meng [57] for exact DNN representation results for certain Hamilton–Jacobi PDEs, and we also refer, e.g., to Geist et al. [81] for numerical investigations regarding the expressive power of DNNs in the context of the approximation of solutions of PDEs.

There are to our best knowledge no results to date rigorously showing for a neural network-based approximation method for PDEs that the optimization error associated to an SGD type method with one random initialization is not subject to the curse of dimensionality, nor that it even converges to zero, except for the special situation where only the parameters in the output layer are learned during training, in which case it has been shown under suitable assumptions that shallow neural networks can learn the solutions to Black–Scholes type PDEs without the curse of dimensionality (see Gonon [93]).

6.2 Approximation error bounds for DNN approximations for nonlinear heat PDEs

In order to provide the reader with a more formal illustration of the type of results obtained in the branch of research outlined in Section 6.1 above, we present in this section in the following theorem, Theorem 6.1 below, a special case of the main result in [131].

Theorem 6.1. *Let $\mathbf{N} = \bigcup_{L \in \mathbb{N}} \bigcup_{l_0, l_1, \dots, l_L \in \mathbb{N}} (\times_{k=1}^L (\mathbb{R}^{l_k \times l_{k-1}} \times \mathbb{R}^{l_k}))$, let $\mathcal{R}: \mathbf{N} \rightarrow (\bigcup_{k, l \in \mathbb{N}} C(\mathbb{R}^k, \mathbb{R}^l))$ and $\mathcal{P}: \mathbf{N} \rightarrow \mathbb{N}$ satisfy for all $L \in \mathbb{N}$, $l_0, l_1, \dots, l_L \in \mathbb{N}$, $\Phi = ((W_1, B_1), (W_2, B_2), \dots, (W_L, B_L)) \in (\times_{k=1}^L (\mathbb{R}^{l_k \times l_{k-1}} \times \mathbb{R}^{l_k}))$, $x_0 \in \mathbb{R}^{l_0}$, $x_1 \in \mathbb{R}^{l_1}$, \dots , $x_L \in \mathbb{R}^{l_L}$ with $\forall k \in \mathbb{N} \cap (0, L): x_k = \mathbf{r}_{l_k}(W_k x_{k-1} + B_k)$ that $\mathcal{R}(\Phi) \in C(\mathbb{R}^{l_0}, \mathbb{R}^{l_L})$, $(\mathcal{R}(\Phi))(x_0) = W_L x_{L-1} + B_L$, and $\mathcal{P}(\Phi) = \sum_{k=1}^L l_k(l_{k-1} + 1)$, let $T, \kappa \in (0, \infty)$, $(\mathbf{g}_{d, \varepsilon})_{(d, \varepsilon) \in \mathbb{N} \times (0, 1]} \subseteq \mathbf{N}$, let $u_d \in C^{1,2}([0, T] \times \mathbb{R}^d, \mathbb{R})$, $d \in \mathbb{N}$, let $f: \mathbb{R} \rightarrow \mathbb{R}$ be Lipschitz continuous, and assume for all $d \in \mathbb{N}$, $x = (x_1, x_2, \dots, x_d) \in \mathbb{R}^d$, $\varepsilon \in (0, 1]$, $t \in [0, T]$ that $\mathcal{R}(\mathbf{g}_{d, \varepsilon}) \in C(\mathbb{R}^d, \mathbb{R})$, $\varepsilon |u_d(t, x)| + |u_d(0, x) - (\mathcal{R}(\mathbf{g}_{d, \varepsilon}))(x)| \leq \varepsilon \kappa d^\kappa (1 + \sum_{i=1}^d |x_i|^\kappa)$, $\mathcal{P}(\mathbf{g}_{d, \varepsilon}) \leq \kappa d^\kappa \varepsilon^{-\kappa}$, and*

$$\frac{\partial u_d}{\partial t}(t, x) = \Delta_x u_d(t, x) + f(u_d(t, x)) \quad (39)$$

(cf. Theorem 2.5). Then there exist $(\mathbf{u}_{d, \varepsilon})_{(d, \varepsilon) \in \mathbb{N} \times (0, 1]} \subseteq \mathbf{N}$ and $c \in \mathbb{R}$ such that for all $d \in \mathbb{N}$, $\varepsilon \in (0, 1]$ it holds that $\mathcal{R}(\mathbf{u}_{d, \varepsilon}) \in C(\mathbb{R}^d, \mathbb{R})$, $\mathcal{P}(\mathbf{u}_{d, \varepsilon}) \leq c d^c \varepsilon^{-c}$, and

$$\left[\int_{[0, 1]^d} |u_d(T, x) - (\mathcal{R}(\mathbf{u}_{d, \varepsilon}))(x)|^2 dx \right]^{1/2} \leq \varepsilon. \quad (40)$$

Theorem 6.1 follows immediately from [131, Theorem 1.1]. In the following we add some comments on the mathematical objects appearing in Theorem 6.1 above. The set \mathbf{N} in Theorem 6.1 represents the set of all neural networks. More specifically, each element $\Phi \in (\times_{k=1}^L (\mathbb{R}^{l_k \times l_{k-1}} \times \mathbb{R}^{l_k}))$ with $L \in \mathbb{N}$, $l_0, l_1, \dots, l_L \in \mathbb{N}$ represents a neural network where $L \in \mathbb{N}$ is the length of the neural network and $l_0, l_1, \dots, l_L \in \mathbb{N}$ correspond to the number of neurons in the 1st, 2nd, \dots , $(L + 1)$ th layer, respectively. The function

$$\mathcal{R}: \mathbf{N} \rightarrow (\bigcup_{k, l \in \mathbb{N}} C(\mathbb{R}^k, \mathbb{R}^l)) \quad (41)$$

in Theorem 6.1 assigns to each neural network its associated realization function. More specifically, for each neural network $\Phi \in \mathbf{N}$ it holds that $\mathcal{R}(\Phi) \in (\bigcup_{k,l \in \mathbb{N}} C(\mathbb{R}^k, \mathbb{R}^l))$ is the realization function of the neural network Φ , where the activation functions are multidimensional versions of the rectifier function introduced in Theorem 2.5 above. The function $\mathcal{P}: \mathbf{N} \rightarrow \mathbb{N}$ assigns to each neural network $\Phi \in \mathbf{N}$ the number of parameters employed in the description of the neural network Φ . We observe that for every $\Phi \in \mathbf{N}$ it holds that $\mathcal{P}(\Phi)$ corresponds, roughly speaking, to the amount of memory necessary to store the neural network Φ on a computer.

In (39) in Theorem 6.1 we specify the PDEs whose solutions we intend to approximate by neural networks. The functions $u_d: [0, T] \times \mathbb{R}^d \rightarrow \mathbb{R}$, $d \in \mathbb{N}$, in Theorem 6.1 denote the exact solutions of the PDEs in (39). The real number $T \in (0, \infty)$ in Theorem 6.1 denotes the time horizon of the PDEs in (39). The function $f: \mathbb{R} \rightarrow \mathbb{R}$ in Theorem 6.1 describes the Lipschitz nonlinearity in the PDEs in (39). The real number $\kappa \in (0, \infty)$ in Theorem 6.1 is a constant used to formulate the regularity and approximation hypotheses in Theorem 6.1. We assume in Theorem 6.1 that the solutions $u_d: [0, T] \times \mathbb{R}^d \rightarrow \mathbb{R}$, $d \in \mathbb{N}$, of the PDEs in (39) grow at most polynomially. The real number $\kappa \in (0, \infty)$ is used to formulate this polynomial growth assumption in Theorem 6.1. More formally, in Theorem 6.1 it is assumed that for all $d \in \mathbb{N}$, $t \in [0, T]$, $x = (x_1, x_2, \dots, x_d) \in \mathbb{R}^d$ it holds that

$$|u_d(t, x)| \leq \kappa d^\kappa (1 + \sum_{k=1}^d |x_k|^\kappa). \quad (42)$$

The neural networks $\mathbf{g}_{d,\varepsilon} \in \mathbf{N}$, $d \in \mathbb{N}$, $\varepsilon \in (0, 1]$, in Theorem 6.1 describe neural network approximations to the initial conditions $\mathbb{R}^d \ni x \mapsto u_d(0, x) \in \mathbb{R}$, $d \in \mathbb{N}$, of the PDEs in (39). In particular, note that the hypothesis in Theorem 6.1 that for all $d \in \mathbb{N}$, $x = (x_1, x_2, \dots, x_d) \in \mathbb{R}^d$, $\varepsilon \in (0, 1]$, $t \in [0, T]$ it holds that

$$\varepsilon |u_d(t, x)| + |u_d(0, x) - (\mathcal{R}(\mathbf{g}_{d,\varepsilon}))(x)| \leq \varepsilon \kappa d^\kappa (1 + \sum_{i=1}^d |x_i|^\kappa) \quad (43)$$

implies that for all $d \in \mathbb{N}$, $x \in \mathbb{R}^d$ it holds that $(\mathcal{R}(\mathbf{g}_{d,\varepsilon}))(x)$ converges to $u_d(0, x)$ as ε tends to 0. Observe that this in combination with the assumption in Theorem 6.1 that for all $d \in \mathbb{N}$, $\varepsilon \in (0, 1]$ it holds that $\mathcal{P}(\mathbf{g}_{d,\varepsilon}) \leq \kappa d^\kappa \varepsilon^{-\kappa}$ ensures that the initial conditions of the PDEs in (39) can be approximated through neural networks without the curse of dimensionality.

Theorem 6.1 establishes that there exist neural networks $\mathbf{u}_{d,\varepsilon} \in \mathbf{N}$, $d \in \mathbb{N}$, $\varepsilon \in (0, 1]$, such that for all $d \in \mathbb{N}$, $\varepsilon \in (0, 1]$ it holds that the L^2 -distance, with respect to the Lebesgue measure on the region $[0, 1]^d$, between the exact solution $\mathbb{R}^d \ni x \mapsto u_d(T, x) \in \mathbb{R}$ of the PDE in (39) at the terminal time $T \in (0, \infty)$ and the realization function $\mathcal{R}(\mathbf{u}_{d,\varepsilon}): \mathbb{R}^d \rightarrow \mathbb{R}$ of the neural network $\mathbf{u}_{d,\varepsilon} \in \mathbf{N}$ is bounded by ε and such that the number of parameters of the neural networks $\mathbf{u}_{d,\varepsilon} \in \mathbf{N}$, $d \in \mathbb{N}$, $\varepsilon \in (0, 1]$, grows at most polynomially in both the PDE dimension $d \in \mathbb{N}$ and the reciprocal $1/\varepsilon$ of the prescribed approximation accuracy $\varepsilon \in (0, 1]$. More precisely, Theorem 6.1 establishes that there exist real numbers $K, c \in \mathbb{R}$ such that it holds for all $d \in \mathbb{N}$, $\varepsilon \in (0, 1]$ that

$$\mathcal{P}(\mathbf{u}_{d,\varepsilon}) \leq K d^c \varepsilon^{-c}. \quad (44)$$

We remark that while the statement of Theorem 6.1 in principle allows both K and c in the claim to depend on the time horizon $T \in (0, \infty)$, we expect that c can in fact be chosen independently of T . In contrast, we expect K to grow exponentially with T (in the absence of additional assumptions), similar to approximations of ODEs by the Euler method (see also [129, Theorem 3.8]). It is conceivable that this dependency could be improved, as in the approximation of ODEs, with additional assumptions, such as dissipativity.

In the following we add some comments on the arguments of the proof of Theorem 6.1. The key idea of the proof of Theorem 6.1 is

- (A) to consider, for every $\varepsilon \in (0, 1]$, perturbed versions of the PDEs in (39) in which the nonlinearity $f: \mathbb{R} \rightarrow \mathbb{R}$ is replaced by the realization of a suitable DNN and in which the initial condition functions $\mathbb{R}^d \ni x \mapsto u_d(0, x) \in \mathbb{R}$, $d \in \mathbb{N}$, are replaced by the realizations $\mathcal{R}(\mathbf{g}_{d,\varepsilon}): \mathbb{R}^d \rightarrow \mathbb{R}$, $d \in \mathbb{N}$, of the given DNNs $\mathbf{g}_{d,\varepsilon} \in \mathbf{N}$, $d \in \mathbb{N}$,
- (B) to approximate the perturbed versions of the PDEs in (39) according to item (A) by means of MLP approximation methods (which are known to overcome the curse of dimensionality in the approximation of nonlinear heat equations with Lipschitz nonlinearities; see, e.g., [129] and Section 1 above), and

- (c) to represent suitable random realizations of these MLP approximations as realization functions of DNNs by mimicking the construction of MLP approximations through DNNs.

We refer to [67, Section 7] for further details and to [131] for the detailed proof of Theorem 6.1.

As indicated in item (B) above, the proof of Theorem 6.1 above crucially uses the fact that MLP approximation algorithms do overcome the curse of dimensionality in the approximative solution of nonlinear heat PDEs with Lipschitz continuous nonlinearities (see [129]). We would like to point out that, while Theorem 6.1 above is a statement about the class of nonlinear heat PDEs with Lipschitz continuous nonlinearities, the fact that MLP approximations overcome the curse of dimensionality has been established for a much larger class of PDEs (see [14] for MLP approximations for heat PDEs with possibly non-Lipschitz continuous nonlinearities; see [13] for MLP approximations for semilinear elliptic PDEs; see [130, 132] for MLP approximations for parabolic PDEs with more general second order differential operators than just the Laplacian; see [133] for MLP approximations for semilinear PDEs with gradient-dependent nonlinearities). These results make it seem feasible that results analogous to Theorem 6.1 above may be established for other classes of PDEs as well.

7 Conclusion

In recent years, deep learning has become a powerful tool for approximating solutions of PDEs, especially in high dimensions. In this article we have focused on describing a selection of deep learning-based approximation methods for high-dimensional PDEs from the literature. We also briefly reviewed the wider field as well as selected other Monte Carlo methods for approximating solutions of high-dimensional PDEs.

We believe that these developments pave the way to an exciting future for this area of research. The tools surveyed here open the door to finding solutions for a range of practically relevant problems that were inaccessible until quite recently. Notably, it has suddenly become feasible to find approximate solutions to semilinear PDEs in 1000 or 10 000 space dimensions (cf., e.g., [10, 17] and Section 5 above), a problem that until a few years ago had to be considered completely out of reach. In our own subjective view, this could, on the one hand, lead to dramatic new approaches in applications, e.g., concerning optimal control problems, concerning nonlinear filtering problems, concerning the approximative pricing of products, and concerning the modelling of complex systems in physics and biology (see Section 1). On the other hand, the developments laid out here open up new paths of research. Firstly, the advances reviewed here will likely spawn new approximation methods for high-dimensional PDEs, which will, secondly, demand rigorous mathematical analyses of their approximative capabilities. In particular, though the results surveyed in Section 6 provide a start to the mathematical analysis of deep learning-based approximation methods for PDEs, there is still a long way to go towards a full mathematical theory. And thirdly, the results surveyed here might have ramifications for a regularity theory for high-dimensional PDEs, where higher regularity does not correspond to higher smoothness properties of the involved functions but where higher regularity corresponds to better approximability properties of the involved functions in high dimensions (cf. Beneventano et al. [24, Section 3]).

8 Source code for simulations

In this appendix we provide the complete source code used to obtain the simulation results in Section 5 above. All of the PYTHON source files listed here can be downloaded as part of the sources of the arXiv version of this article at <https://arxiv.org/e-print/2012.12348> (in the form of a gzipped tar file).

8.1 Common source code

```
1 import time
```

```

2 import json
3 import math
4 import logging
5
6 from collections import namedtuple
7
8 JobConfig = namedtuple('JobConfig', ['build_model', 'runs', 'train',
9                                     'train_params', 'evaluate'])
10
11 JobResult = namedtuple('JobResult', ['model', 'values', 'train_times'])
12
13 def run_job(job_config):
14     values = []
15     train_times = []
16
17     model = job_config.build_model()
18
19     for run in range(job_config.runs):
20         logging.debug(f"Starting Run {run+1}")
21
22         tick = time.perf_counter()
23         job_config.train(model, job_config.train_params)
24         tock = time.perf_counter()
25
26         value = job_config.evaluate(model)
27
28         values.append(value)
29         train_times.append(tock - tick)
30
31         logging.debug(f"Value: {value}")
32         logging.debug(f"Time: {tock - tick}\n")
33
34     return JobResult(model, values, train_times)
35
36
37 def run_jobs(job_configs, init, report):
38     results = []
39
40     for config in job_configs:
41         init()
42
43         for (k,v) in config.train_params.items():
44             logging.info(f"{k}: {v}")
45             logging.info("")
46
47         result = run_job(config)
48         results.append(report(result, config.train_params))
49
50     return results
51
52
53 def report(job_result, train_params):
54     mean = sum(job_result.values) / len(job_result.values)
55     result = {
56         "values": job_result.values,
57         "train_times": job_result.train_times,
58         "model": f"{job_result.model}",
59         "mean": mean,
60         "stddev": math.sqrt(sum([(y - mean)**2 for y in job_result.values])
61                               / len(job_result.values)),
62         "avgruntime": sum(job_result.train_times) / len(job_result.train_times),
63         "train_params": {k:v for (k,v) in train_params.items()
64                          if isinstance(v, (int, str, float))}
65     }
66
67     logging.info(f"Mean: {result['mean']}")
68     logging.info(f"Std dev: {result['stddev']}")
69     logging.info(f"Avg runtime: {result['avgruntime']}")
70     logging.info("\n-----\n")
71

```

```

72     return result
73
74
75 def write_results(results, filename):
76     with open(filename, mode="w") as file:
77         json.dump(results, file, indent=4)

```

Source Code 4: The source code for util.py, a PYTHON module containing utility functions used for running the simulations.

8.2 Source code for the deep Galerkin method

```

1  import torch
2
3  # Computes an approximation of  $\mathbb{E}[|v(0,X) - \varphi(X)|^2]$  using the rows of x as independent
4  # realizations of the random variable X
5  def dgm_initial_loss(v,  $\varphi$ , x, dev):
6      t = torch.zeros(x.shape[0],1).to(dev)
7      u = v(torch.cat((t,x), axis=1))
8      return (u -  $\varphi$ (x)).square().mean()
9
10 # Computes an approximation of  $\mathbb{E}[|\partial v/\partial t(T,X) - \Delta_x v(T,X) - f(v(T,X))|^2]$  using the
11 # rows of t and x as independent realizations of the random variables T and X,
12 # respectively
13 def dgm_dynamic_loss(v,  $\rho$ , f, t, x, dev):
14     d = x.shape[1]
15
16     # Split x up into components
17     x_comp = [x[:,i] for i in range(d)]
18
19     # Compute v(t,x)
20     u = v(torch.stack([t] + x_comp, 1))
21
22     # Compute  $\partial v/\partial t(t,x)$ 
23     u_t = torch.autograd.grad(u, t, torch.ones_like(u), create_graph=True)[0]
24
25     # Compute  $\Delta_x v(t,x)$ 
26      $\Delta u$  = torch.zeros(x.shape[0]).to(dev)
27     for i in range(d):
28         # Compute  $\partial v/\partial x_i(x,t)$ 
29         u_xi = torch.autograd.grad(u, x_comp[i], torch.ones_like(u),
30                                     create_graph=True)[0]
31         # Compute  $\partial^2 v/\partial x_i^2(x,t)$ 
32         u_xixi = torch.autograd.grad(u_xi, x_comp[i], torch.ones_like(u_xi),
33                                       create_graph=True)[0]
34          $\Delta u$  += u_xixi
35
36     return (u_t -  $\rho$ *  $\Delta u$  - f(u)).square().mean()
37
38 # Applies Xavier initialization to the module m (if it is a Linear module)
39 def init_weights(m):
40     if isinstance(m, torch.nn.Linear):
41         torch.nn.init.xavier_uniform_(m.weight)
42         torch.nn.init.normal_(m.bias, std=0.1)
43
44 def train( $\varphi$ ,  $\rho$ , f, d, T, model, steps, batch_size, lr, stddev, lr_decay, dev):
45     with torch.no_grad():
46         # Initialize the weights and biases
47         model.apply(init_weights)
48         # Set up the Adam optimizer
49         optimizer = torch.optim.Adam(model.parameters(), lr=lr)
50         # Set up the exponential learning rate decay
51         scheduler = torch.optim.lr_scheduler.ExponentialLR(optimizer, lr_decay)
52
53     for step in range(steps):
54         with torch.no_grad():

```



```

55         # Generate the collocation points
56         sd = stddev((steps - step) / steps)
57         x = (torch.randn(batch_size,d) * sd).to(dev)
58         x.requires_grad_()
59         t = T * torch.rand(batch_size).to(dev)
60         t.requires_grad_()
61
62         optimizer.zero_grad()
63         # Compute the loss
64         initial_loss = dgm_initial_loss(model,  $\phi$ , x, dev)
65         dynamic_loss = dgm_dynamic_loss(model,  $\rho$ , f, t, x, dev)
66         loss = initial_loss + dynamic_loss
67         # Compute the gradients
68         loss.backward()
69         # Apply the change to the weights and biases of model
70         optimizer.step()
71         # Decrease the learning rate
72         scheduler.step()

```

Source Code 5: The source code for `dgm.py`, a PYTHON module containing the core of the implementation of the deep Galerkin method.

```

1  import torch
2
3  # Returns a fully connected feed-forward model with the given layer
4  # dimensions in which the affine transformation in each hidden layer
5  # is followed by the given activation function
6  def build_model(dev, activation, *layer_dims):
7      return lambda: torch.nn.Sequential(
8          *[l for (i, j) in zip(layer_dims, layer_dims[1:-1])
9              for l in [torch.nn.Linear(i,j), activation()]],
10         torch.nn.Linear(layer_dims[-2], layer_dims[-1])
11     ).to(dev)

```

Source Code 6: The source code for `dgm_util.py`, a PYTHON module containing a utility function for building the DNNs used in the simulations for the deep Galerkin method.

```

1  import sys
2  import logging
3  import torch
4
5  from dgm import train
6  from util import JobConfig, run_jobs, report, write_results
7  from dgm_util import build_model
8
9  # Use the GPU if available
10 dev = torch.device("cuda" if torch.cuda.is_available() else "cpu")
11
12 T = .5
13  $\rho$  = 1.
14
15 # The initial values of the PDE
16 def  $\phi_1(x)$ :
17     return (1. + x.square()).sum(axis=1, keepdim=True)).sqrt()
18
19 def  $\phi_2(x)$ :
20     return 2. / (4. + x.square()).sum(axis=1, keepdim=True))
21
22 def  $\phi_3(x)$ :
23     return torch.atan(x.square()).sum(axis=1, keepdim=True).sqrt() / 2.)
24
25 # The nonlinearity of the PDE
26 def f(y):
27     return torch.sin(y)

```

```

28
29 def evaluator(d):
30     return lambda model: model(torch.tensor([[T] + [0.0] * d]).to(dev)).item()
31
32 configs1 = [
33     JobConfig(
34         build_model = build_model(dev, torch.nn.Mish, d + 1, d + 40, d + 40,
35                                   d + 40, 1),
36         runs = 20,
37         train = lambda model, train_params:
38             train(φ1, ρ, f, model=model, dev=dev, **train_params),
39         train_params = {
40             "d": d,
41             "T": T,
42             "steps": 350 if d<20 else
43                     500 if d<50 else
44                     750,
45             "batch_size": 256,
46             "lr": 0.05 if d<20 else
47                  0.025 if d<50 else
48                  0.01 if d<200 else
49                  0.005,
50             "lr_decay": 0.98 if d<20 else
51                        0.99 if d<50 else
52                        0.995,
53             "stddev": lambda p: 2**(3. * p -.5)
54         },
55         evaluate = evaluator(d)
56     ) for d in [1, 2, 5, 10, 20, 50, 100, 200]
57 ]
58
59 configs2 = [
60     JobConfig(
61         build_model = build_model(dev, torch.nn.Mish, d + 1, d + 40, d + 40,
62                                   d + 40, 1),
63         runs = 20,
64         train = lambda model, train_params:
65             train(φ2, ρ, f, model=model, dev=dev, **train_params),
66         train_params = {
67             "d": d,
68             "T": T,
69             "steps": 500 if d<10 else
70                     750 if d<50 else
71                     1000,
72             "batch_size": 256,
73             "lr": 0.05 if d<10 else
74                  0.025 if d<50 else
75                  0.01 if d<200 else
76                  0.005,
77             "lr_decay": 0.99 if d<10 else
78                        0.995 if d<50 else
79                        0.998,
80             "stddev": lambda p: 2**(3. * p -.5)
81         },
82         evaluate = evaluator(d)
83     ) for d in [1, 2, 5, 10, 20, 50, 100, 200]
84 ]
85
86 configs3 = [
87     JobConfig(
88         build_model = build_model(dev, torch.nn.Mish, d + 1, d + 40, d + 40,
89                                   d + 40, 1),
90         runs = 20,
91         train = lambda model, train_params:
92             train(φ2, ρ, f, model=model, dev=dev, **train_params),
93         train_params = {
94             "d": d,
95             "T": T,
96             "steps": 350 if d<20 else
97                     500 if d<50 else

```

```

98         750,
99         "batch_size": 256,
100        "lr": 0.05 if d<20 else
101            0.025 if d<50 else
102            0.01 if d<200 else
103            0.005,
104        "lr_decay": 0.98 if d<20 else
105                    0.99 if d<50 else
106                    0.995,
107        "stddev": lambda p: 2**(3. * p -.5)
108    },
109    evaluate = evaluator(d)
110    ) for d in [1, 2, 5, 10, 20, 50, 100, 200]
111 ]
112
113 logging.basicConfig(format='%(message)s', level=logging.DEBUG, stream=sys.stdout)
114
115 results1 = run_jobs(configs1, lambda: torch.manual_seed(0), report)
116 write_results(results1, "dgm_1.json")
117
118 results2 = run_jobs(configs2, lambda: torch.manual_seed(0), report)
119 write_results(results2, "dgm_2.json")
120
121 results3 = run_jobs(configs3, lambda: torch.manual_seed(0), report)
122 write_results(results3, "dgm_3.json")

```

Source Code 7: The source code for `dgm_examples.py`, a PYTHONscript that runs the simulations for the deep Galerkin method and writes the results to files.

8.3 Source code for the deep splitting method

```

1  import torch
2  import math
3
4  # Computes an approximation of  $\mathbb{E}[\|\varphi(\sqrt{(2\rho T)} W + \xi) + Tf(\varphi(\sqrt{(2\rho T)} W + \xi)) - N(\xi)\|^2]$ 
5  # with  $W$  a standard normal random variable using the rows of  $x$  as independent
6  # realizations of the random variable  $\xi$ 
7  def loss( $\varphi$ ,  $\rho$ , model, f, T, x, dev):
8      with torch.no_grad():
9          W = torch.randn_like(x).to(dev)
10         z =  $\varphi(x + \text{math.sqrt}(2 * \rho * T) * W)$ 
11         y = z + T * f(z)
12         return (y - model(x)).square().mean()
13
14  # Applies Xavier initialization to the module m (if it is a Linear module)
15  def init_weights(m):
16      if isinstance(m, torch.nn.Linear):
17          torch.nn.init.xavier_uniform_(m.weight)
18          torch.nn.init.normal_(m.bias)
19
20  def train( $\varphi$ ,  $\rho$ , f, d, T, models, lr, lr_decay, steps, batch_size, dev):
21      n = len(models)
22      for i in range(n):
23          # Train model[i]
24          with torch.no_grad():
25              # Initialize the weights and biases
26              models[i].apply(init_weights)
27              # Set up the Adam optimizer
28              optimizer = torch.optim.Adam(models[i].parameters(), lr=lr)
29              # Set up the exponential learning rate decay
30              scheduler = torch.optim.lr_scheduler.ExponentialLR(optimizer, lr_decay)
31
32          models[i].train()
33          for step in range(steps):

```

```

34         # Generate the collocation points
35         with torch.no_grad():
36             x = math.sqrt(2 * (n-i-1) * T/n) * torch.randn(batch_size, d).to(dev)
37         optimizer.zero_grad()
38         # Compute the loss
39         loss_value = loss( $\phi$  if i==0 else models[i-1],  $\rho$ , models[i], f, T/n, x, dev)
40         # Compute the gradients
41         loss_value.backward()
42         # Apply changes to weights and biases of model[i]
43         optimizer.step()
44         # Decrease the learning rate
45         scheduler.step()
46
47     models[i].eval()

```

Source Code 8: The source code for `ds.py`, a PYTHON module containing the core of the implementation of the deep splitting method.

```

1  import torch
2
3  # Returns a list of N fully connected feed-forward models. The first N-1 models have
4  # the given layer dimensions, in which the affine transformation in each hidden layer
5  # is followed by the given activation function. Optionally batch normalization is
6  # inserted before each activation function. The N-th model is a single affine linear
7  # transformation.
8  def build_models(dev, N, activation, batch_normalization, *layer_dims):
9      def builder():
10         stages = [(
11             torch.nn.Linear(i,j),
12             *((torch.nn.BatchNorm1d(j),) if batch_normalization else ()),
13             activation()
14         ) for (i, j) in zip(layer_dims, layer_dims[1:-1])
15         ] for _ in range(N-1)]
16         return [torch.nn.Sequential(
17             *[m for stage in stages[i] for m in stage],
18             torch.nn.Linear(layer_dims[-2], layer_dims[-1]),
19             *((torch.nn.BatchNorm1d(layer_dims[-1]),) if batch_normalization else ()),
20         ).to(dev)
21         for i in range(N-1)
22         ] + [torch.nn.Linear(layer_dims[0], layer_dims[-1]).to(dev)]
23     return builder

```

Source Code 9: The source code for `ds_util.py`, a PYTHON module containing a utility function for building the DNNs used in the simulations for the deep splitting method.

```

1  import sys
2  import logging
3  import torch
4
5  from ds import train
6  from util import JobConfig, run_jobs, report, write_results
7  from ds_util import build_models
8
9  # Use the GPU if available
10 dev = torch.device("cuda" if torch.cuda.is_available() else "cpu")
11
12 T = .5
13  $\rho$  = 1.
14
15 # The initial values of the PDE
16 def  $\phi_1(x)$ :
17     return (1. + x.square()).sum(axis=1, keepdim=True)).sqrt()
18
19 def  $\phi_2(x)$ :

```

```

20     return 2. / (4. + x.square().sum(axis=1, keepdim=True))
21
22 def  $\phi_3(x)$ :
23     return torch.atan(x.square().sum(axis=1, keepdim=True).sqrt() / 2.)
24
25 # The nonlinearity of the PDE
26 def f(y):
27     return torch.sin(y)
28
29 def evaluator(d):
30     return lambda models: models[-1](torch.zeros(1,d).to(dev)).item()
31
32 def train_params(d):
33     return {
34         "d": d,
35         "T": T,
36         "steps": 350 if d<20 else
37                 500 if d<100 else
38                 750 if d<200 else
39                 1000 if d<1000 else
40                 1250,
41         "batch_size": 256,
42         "lr": 0.2,
43         "lr_decay": 0.985 if d<20 else
44                    0.99 if d<100 else
45                    0.995 if d<1000 else
46                    0.998
47     }
48
49 def trainer( $\phi$ ):
50     return lambda models, train_params: train( $\phi$ ,  $\rho$ , f, models=models,
51                                               dev=dev, **train_params)
52
53 configs = [
54     [
55         JobConfig(
56             build_model =
57                 build_models(dev, 30, torch.nn.ELU, True, d, d + 50, d + 50, 1),
58             runs = 20,
59             train = trainer( $\phi$ ),
60             train_params = train_params(d),
61             evaluate = evaluator(d)
62         ) for d in [1, 2, 5, 10, 20, 50, 100, 200, 500, 1000]
63     ] for  $\phi$  in [ $\phi_1$ ,  $\phi_2$ ,  $\phi_3$ ]
64 ]
65
66 logging.basicConfig(format='%(message)s', level=logging.DEBUG, stream=sys.stdout)
67
68 results1 = run_jobs(configs[0], lambda: torch.manual_seed(0), report)
69 write_results(results1, "ds_1.json")
70
71 results2 = run_jobs(configs[1], lambda: torch.manual_seed(0), report)
72 write_results(results2, "ds_2.json")
73
74 results3 = run_jobs(configs[2], lambda: torch.manual_seed(0), report)
75 write_results(results3, "ds_3.json")

```

Source Code 10: The source code for `ds_examples.py`, a PYTHON script that runs the simulations for the deep splitting method and writes the results to files.

Acknowledgements

This work has been funded by the Deutsche Forschungsgemeinschaft (DFG, German Research Foundation) under Germany's Excellence Strategy EXC 2044 – 390685587, Mathematics Münster: Dynamics – Geometry – Structure and through the research grant HU1889/7-1. This project has been partially supported by the startup fund project of Shenzhen Research Institute of Big Data under grant No. T00120220001.

References

- [1] ABBAS-TURKI, L., DIALLO, B., AND PAGÈS, G. Conditional Monte Carlo Learning for Diffusions I: main methodology and application to backward stochastic differential equations. *Preprint available at <https://hal.archives-ouvertes.fr/hal-02959492>* (2020), 28 pages.
- [2] ABBAS-TURKI, L., DIALLO, B., AND PAGÈS, G. Conditional Monte Carlo Learning for Diffusions II: extended methodology and application to risk measures and early stopping problems. *Preprint available at <https://hal.archives-ouvertes.fr/hal-02959494>* (2020), 31 pages.
- [3] AL-ARADI, A., CORREIA, A., JARDIM, G., DE FREITAS NAIFF, D., AND SAPORITO, Y. Extensions of the deep Galerkin method. *Appl. Math. Comput.* **430** (2022), 127287.
- [4] ANDERSSON, K., ANDERSSON, A., AND OOSTERLEE, C. W. Convergence of a robust deep FBSDE method for stochastic control. *arXiv:2201.06854* (2022), 27 pages.
- [5] ANITESCU, C., ATROSHCHENKO, E., ALAJLAN, N., AND RABCZUK, T. Artificial neural network methods for the solution of second order boundary value problems. *Comput. Mater. Contin.* **59**, 1 (2019), 345–359.
- [6] BALLY, V., AND PAGÈS, G. Error analysis of the optimal quantization algorithm for obstacle problems. *Stochastic Process. Appl.* **106**, 1 (2003), 1–40.
- [7] BALLY, V., AND PAGÈS, G. A quantization algorithm for solving multi-dimensional discrete-time optimal stopping problems. *Bernoulli* **9**, 6 (2003), 1003–1049.
- [8] BAYER, C., QIU, J., AND YAO, Y. Pricing options under rough volatility with backward SPDEs. *SIAM J. Financial Math.* **13**, 1 (2022), 179–212.
- [9] BECK, C., BECKER, S., CHERIDITO, P., JENTZEN, A., AND NEUFELD, A. Deep learning based numerical approximation algorithms for stochastic partial differential equations and high-dimensional nonlinear filtering problems. *arXiv:2012.01194* (2020), 58 pages.
- [10] BECK, C., BECKER, S., CHERIDITO, P., JENTZEN, A., AND NEUFELD, A. Deep splitting method for parabolic PDEs. *SIAM J. Sci. Comput.* **43**, 5 (2021), A3135–A3154.
- [11] BECK, C., BECKER, S., GROHS, P., JAAFARI, N., AND JENTZEN, A. Solving the Kolmogorov PDE by means of deep learning. *J. Sci. Comput.* **88**, 3 (2021), Paper no. 73, 28 pp.
- [12] BECK, C., E, W., AND JENTZEN, A. Machine learning approximation algorithms for high-dimensional fully nonlinear partial differential equations and second-order backward stochastic differential equations. *J. Nonlinear Sci.* **29**, 4 (2019), 1563–1619.
- [13] BECK, C., GONON, L., AND JENTZEN, A. Overcoming the curse of dimensionality in the numerical approximation of high-dimensional semilinear elliptic partial differential equations. *arXiv:2003.00596* (2020), 50 pages.
- [14] BECK, C., HORNUNG, F., HUTZENTHALER, M., JENTZEN, A., AND KRUSE, T. Overcoming the curse of dimensionality in the numerical approximation of Allen–Cahn partial differential equations via truncated full-history recursive multilevel Picard approximations. *J. Numer. Math.* **28**, 4 (2020), 197–222.
- [15] BECK, C., HUTZENTHALER, M., AND JENTZEN, A. On nonlinear Feynman–Kac formulas for viscosity solutions of semilinear parabolic partial differential equations. *Stoch. Dyn.* **21**, 8 (2021), Paper no. 2150048, 68 pp.
- [16] BECK, C., JENTZEN, A., AND KRUSE, T. Nonlinear Monte Carlo methods with polynomial runtime for high-dimensional iterated nested expectations. *arXiv:2009.13989* (2020), 47 pages.

- [17] BECKER, S., BRAUNWARTH, R., HUTZENTHALER, M., JENTZEN, A., AND VON WURSTEMBERGER, P. Numerical simulations for full history recursive multilevel Picard approximations for systems of high-dimensional partial differential equations. *Commun. Comput. Phys.* 28, 5 (2020), 2109–2138.
- [18] BECKER, S., CHERIDITO, P., AND JENTZEN, A. Deep optimal stopping. *J. Mach. Learn. Res.* 20, 74 (2019), 1–25.
- [19] BECKER, S., CHERIDITO, P., JENTZEN, A., AND WELTI, T. Solving high-dimensional optimal stopping problems using deep learning. *European J. Appl. Math.* 32, 3 (2021), 470–514.
- [20] BECKER, S., JENTZEN, A., MÜLLER, M. S., AND VON WURSTEMBERGER, P. Learning the random variables in Monte Carlo simulations with stochastic gradient descent: Machine learning for parametric PDEs and financial derivative pricing. *arXiv:2002.02717* (2022), 70 pages.
- [21] BENDER, C., AND DENK, R. A forward scheme for backward SDEs. *Stochastic Process. Appl.* 117, 12 (2007), 1793–1812.
- [22] BENDER, C., AND STEINER, J. Least-squares Monte Carlo for backward SDEs. In *Numerical methods in finance*. Springer, 2012, pp. 257–289.
- [23] BENDER, C., AND ZHANG, J. Time discretization and Markovian iteration for coupled FBSDEs. *Ann. Appl. Probab.* 18, 1 (2008), 143–177.
- [24] BENEVENTANO, P., CHERIDITO, P., JENTZEN, A., AND VON WURSTEMBERGER, P. High-dimensional approximation spaces of artificial neural networks and applications to partial differential equations. *arXiv:2012.04326* (2020), 32 pages.
- [25] BERG, J., AND NYSTRÖM, K. A unified deep artificial neural network approach to partial differential equations in complex geometries. *Neurocomputing* 317 (2018), 28–41.
- [26] BERNER, J., GROHS, P., AND JENTZEN, A. Analysis of the generalization error: empirical risk minimization over deep artificial neural networks overcomes the curse of dimensionality in the numerical approximation of Black-Scholes partial differential equations. *SIAM J. Math. Data Sci.* 2, 3 (2020), 631–657.
- [27] BERRONE, S., CANUTO, C., AND PINTORE, M. Solving PDEs by variational physics-informed neural networks: an a posteriori error analysis. *Ann. Univ. Ferrara Sez. VII Sci. Mat.* 68, 2 (Nov 2022), 575–595.
- [28] BERRONE, S., CANUTO, C., AND PINTORE, M. Variational physics informed neural networks: the role of quadratures and test functions. *J. Sci. Comput.* 92, 3 (Aug 2022), 100.
- [29] BLECHSCHMIDT, J., AND ERNST, O. G. Three ways to solve partial differential equations with neural networks — a review. *GAMM-Mitt.* 44, 2 (2021), e202100006.
- [30] BOUCHARD, B., AND TOUZI, N. Discrete-time approximation and Monte-Carlo simulation of backward stochastic differential equations. *Stochastic Process. Appl.* 111, 2 (2004), 175–206.
- [31] BOUSSANGE, V., BECKER, S., JENTZEN, A., KUCKUCK, B., AND PELLISSIER, L. Deep learning approximations for non-local nonlinear PDEs with Neumann boundary conditions. *arXiv:2205.03672* (2020), 59 pages.
- [32] BRANDSTETTER, J., VAN DEN BERG, R., WELLING, M., AND GUPTA, J. K. Clifford neural layers for PDE modeling. *arXiv:2209.04934* (2022), 52 pages.
- [33] BRIAND, P., DELYON, B., AND MÉMIN, J. Donsker-type theorem for BSDEs. *Electron. Commun. Probab.* 6 (2001), 1–14.

- [34] BRIAND, P., AND LABART, C. Simulation of BSDEs by Wiener chaos expansion. *Ann. Appl. Probab.* 24, 3 (06 2014), 1129–1171.
- [35] CAI, S., MAO, Z., WANG, Z., YIN, M., AND KARNIADAKIS, G. E. Physics-informed neural networks (PINNs) for fluid mechanics: a review. *Acta Mech. Sin.* 37, 12 (Dec 2021), 1727–1738.
- [36] CAI, S., WANG, Z., WANG, S., PERDIKARIS, P., AND KARNIADAKIS, G. E. Physics-Informed Neural Networks for Heat Transfer Problems. *J. Heat Transfer* 143, 6 (04 2021), 060801.
- [37] CAI, Z., AND LIU, J. Approximating quantum many-body wave functions using artificial neural networks. *Phys. Rev. B* 97, 3 (2018), 035116.
- [38] CARLEO, G., AND TROYER, M. Solving the quantum many-body problem with artificial neural networks. *Science* 355, 6325 (2017), 602–606.
- [39] CARMONA, R., AND LAURIÈRE, M. Convergence Analysis of Machine Learning Algorithms for the Numerical Solution of Mean Field Control and Games: II – The Finite Horizon Case. *arXiv:1908.01613* (2019), 39 pages.
- [40] CARMONA, R., AND LAURIÈRE, M. Convergence analysis of machine learning algorithms for the numerical solution of mean field control and games I: The ergodic case. *SIAM J. Numer. Anal.* 59, 3 (2021), 1455–1485.
- [41] CASTRO, J. Deep learning schemes for parabolic nonlocal integro-differential equations. *Partial Differ. Equ. Appl.* 3, 6 (Oct 2022), 77.
- [42] CHAN-WAI-NAM, Q., MIKAEL, J., AND WARIN, X. Machine learning for semi linear PDEs. *J. Sci. Comput.* 79, 3 (2019), 1667–1712.
- [43] CHANG, D., LIU, H., AND XIONG, J. A branching particle system approximation for a class of FBSDEs. *Prob. Uncertain. Quant. Risk* 1, 9 (2016), 1–34.
- [44] CHASSAGNEUX, J.-F., AND GARCIA TRILLOS, C. Cubature method to solve BSDEs: Error expansion and complexity control. *Math. Comput.* 89, 324 (2020), 1895–1932.
- [45] CHASSAGNEUX, J.-F., AND RICHOU, A. Numerical stability analysis of the Euler scheme for BSDEs. *SIAM J. Numer. Anal.* 53, 2 (2015), 1172–1193.
- [46] CHEN, F., SONDAK, D., PROTOPAPAS, P., MATTHEAKIS, M., LIU, S., AGARWAL, D., AND DI GIOVANNI, M. NeuroDiffEq: A Python package for solving differential equations with neural networks. *J. Open Source Softw.* 5, 46 (2020), 1931.
- [47] CHEN, Y., LU, L., KARNIADAKIS, G. E., AND DAL NEGRO, L. Physics-informed neural networks for inverse problems in nano-optics and metamaterials. *Opt. Express* 28, 8 (2020), 11618–11633.
- [48] CHEN, Y., AND WAN, J. W. L. Deep neural network framework based on backward stochastic differential equations for pricing and hedging american options in high dimensions. *Quant. Finance* 21, 1 (2021), 45–67.
- [49] CHERIDITO, P., AND STADJE, M. BSDEs and BSDEs with non-Lipschitz drivers: comparison, convergence and robustness. *Bernoulli* 19, 3 (2013), 1047–1085.
- [50] CLEVERT, D.-A., UNTERTHINER, T., AND HOCHREITER, S. Fast and accurate deep network learning by exponential linear units (ELUs). *arXiv:1511.07289* (2015), 14 pages.
- [51] COX, S., AND VAN NEERVEN, J. Pathwise Hölder convergence of the implicit-linear Euler scheme for semi-linear SPDEs with multiplicative noise. *Numer. Math.* 125, 2 (2013), 259–345.

- [52] CRISAN, D., AND MANOLARAKIS, K. Solving backward stochastic differential equations using the cubature method: Application to nonlinear pricing. *SIAM J. Financial Math.* 3, 1 (2012), 534–571.
- [53] CRISAN, D., AND MANOLARAKIS, K. Second order discretization of backward SDEs and simulation with the cubature method. *Ann. Appl. Probab.* 24, 2 (2014), 652–678.
- [54] CRISAN, D., MANOLARAKIS, K., AND TOUZI, N. On the Monte Carlo simulation of BSDEs: An improvement on the Malliavin weights. *Stochastic Process. Appl.* 120, 7 (2010), 1133–1158.
- [55] CUOMO, S., SCHIANO DI COLA, V., GIAMPAOLO, F., ROZZA, G., RAISSI, M., AND PICCIALLI, F. Scientific Machine Learning through Physics-Informed Neural Networks: Where we are and What’s next. *arXiv:2201.05624* (2022), 85 pages.
- [56] DARBON, J., LANGLOIS, G. P., AND MENG, T. Overcoming the curse of dimensionality for some Hamilton-Jacobi partial differential equations via neural network architectures. *Res. Math. Sci.* 7, 3 (2020), Paper No. 20.
- [57] DARBON, J., AND MENG, T. On some neural network architectures that can represent viscosity solutions of certain high dimensional Hamilton-Jacobi partial differential equations. *J. Comput. Phys.* 425 (2021), 109907.
- [58] DARBON, J., AND OSHER, S. Algorithms for overcoming the curse of dimensionality for certain Hamilton-Jacobi equations arising in control theory and elsewhere. *Res. Math. Sci.* 3, 19 (2016).
- [59] DE RAYNAL, P. C., AND TRILLOS, C. G. A cubature based algorithm to solve decoupled McKean-Vlasov forward-backward stochastic differential equations. *Stochastic Process. Appl.* 125, 6 (2015), 2206–2255.
- [60] DELARUE, F., AND MENOZZI, S. A forward-backward stochastic algorithm for quasi-linear PDEs. *Ann. Appl. Probab.* (2006), 140–184.
- [61] DELARUE, F., AND MENOZZI, S. An interpolated stochastic algorithm for quasi-linear PDEs. *Math. Comput.* 77, 261 (2008), 125–158.
- [62] DEVENEY, T., MUELLER, E., AND SHARDLOW, T. A deep surrogate approach to efficient Bayesian inversion in PDE and integral equation models. *arXiv:1910.01547* (2020), 29 pages.
- [63] DISSANAYAKE, M. W. M. G., AND PHAN-THIEN, N. Neural-network-based approximations for solving partial differential equations. *Commun. Numer. Methods Engrg.* 10, 3 (1994), 195–201.
- [64] DOCKHORN, T. A discussion on solving partial differential equations using neural networks. *arXiv:1904.07200* (2019), 9 pages.
- [65] DOLGOV, S., KALISE, D., AND KUNISCH, K. K. Tensor decomposition methods for high-dimensional Hamilton-Jacobi-Bellman equations. *SIAM J. Sci. Comput.* 43, 3 (2021), A1625–A1650.
- [66] E, W., HAN, J., AND JENTZEN, A. Deep learning-based numerical methods for high-dimensional parabolic partial differential equations and backward stochastic differential equations. *Commun. Math. Stat.* 5, 4 (2017), 349–380.
- [67] E, W., HAN, J., AND JENTZEN, A. Algorithms for solving high dimensional PDEs: from nonlinear Monte Carlo to machine learning. *Nonlinearity* 35, 1 (2022), 278–310.
- [68] E, W., HUTZENTHALER, M., JENTZEN, A., AND KRUSE, T. On multilevel Picard numerical approximations for high-dimensional nonlinear parabolic partial differential equations and high-dimensional nonlinear backward stochastic differential equations. *J. Sci. Comput.* 79, 3 (2019), 1534–1571.

- [69] E, W., HUTZENTHALER, M., JENTZEN, A., AND KRUSE, T. Multilevel Picard iterations for solving smooth semilinear parabolic heat equations. *Partial Differ. Equ. Appl.* 2, 6 (2021), Paper no. 80.
- [70] E, W., AND YU, B. The Deep Ritz method: A deep learning-based numerical algorithm for solving variational problems. *Commun. Math. Stat.* 6, 1 (2018), 1–12.
- [71] EIGEL, M., PFEFFER, M., AND SCHNEIDER, R. Adaptive stochastic Galerkin FEM with hierarchical tensor representations. *Numer. Math.* 136, 3 (2017), 765–803.
- [72] ELBRÄCHTER, D., GROHS, P., JENTZEN, A., AND SCHWAB, C. DNN Expression Rate Analysis of High-dimensional PDEs: Application to Option Pricing. *Constr. Approx.* 55 (2022), 3–71.
- [73] FAN, Y., AND YING, L. Solving electrical impedance tomography with deep learning. *J. Comput. Phys.* 404 (2020), 109119.
- [74] FAN, Y., AND YING, L. Solving inverse wave scattering with deep learning. *Ann. Math. Sci. Appl.* 7, 1 (2022), 23–48.
- [75] FREY, R., AND KÖCK, V. Deep neural network algorithms for parabolic PIDEs and applications in insurance mathematics. In *Mathematical and Statistical Methods for Actuarial Sciences and Finance* (Cham, 2022), M. Corazza, C. Perna, C. Pizzi, and M. Sibillo, Eds., Springer International Publishing, pp. 272–277.
- [76] FU, Y., ZHAO, W., AND ZHOU, T. Multistep schemes for forward backward stochastic differential equations with jumps. *J. Sci. Comput.* 69, 2 (2016), 651–672.
- [77] FUJII, M., TAKAHASHI, A., AND TAKAHASHI, M. Asymptotic expansion as prior knowledge in deep learning method for high dimensional BSDEs. *Asia-Pac. Financ. Markets* 26, 3 (2019), 391–408.
- [78] GEISS, C., AND LABART, C. Simulation of BSDEs with jumps by Wiener Chaos expansion. *Stochastic Process. Appl.* 126, 7 (2016), 2123 – 2162.
- [79] GEISS, C., LABART, C., AND LUOTO, A. Mean square rate of convergence for random walk approximation of forward-backward SDEs. *Adv. in Appl. Probab.* 52, 3 (2020), 735–771.
- [80] GEISS, C., LABART, C., AND LUOTO, A. Random walk approximation of BSDEs with Hölder continuous terminal condition. *Bernoulli* 26, 1 (2020), 159–190.
- [81] GEIST, M., PETERSEN, P., RASLAN, M., SCHNEIDER, R., AND KUTYNIOK, G. Numerical solution of the parametric diffusion equation by deep neural networks. *J. Sci. Comput.* 88, 1 (2021), Paper No. 22, 37.
- [82] GERMAIN, M., PHAM, H., AND WARIN, X. Approximation error analysis of some deep backward schemes for nonlinear PDEs. *SIAM J. Sci. Comput.* 44, 1 (2022), A28–A56.
- [83] GILES, M. B. Multilevel Monte Carlo path simulation. *Oper. Res.* 56, 3 (2008), 607–617.
- [84] GILES, M. B. Multilevel Monte Carlo methods. *Acta Numer.* 24 (2015), 259–328.
- [85] GILES, M. B., JENTZEN, A., AND WELTI, T. Generalised multilevel Picard approximations. *arXiv:1911.03188* (2019), 61 pages.
- [86] GLOROT, X., AND BENGIO, Y. Understanding the difficulty of training deep feedforward neural networks. In *Proceedings of the thirteenth international conference on artificial intelligence and statistics* (2010), JMLR Workshop and Conference Proceedings, pp. 249–256.
- [87] GOBET, E., AND LABART, C. Solving BSDE with adaptive control variate. *SIAM J. Numer. Anal.* 48, 1 (2010), 257–277.

- [88] GOBET, E., AND LEMOR, J.-P. Numerical simulation of BSDEs using empirical regression methods: theory and practice. In *5th Colloquium on BSDEs* (Shanghai, Chine, May 2006), S. Tang and S. Peng, Eds.
- [89] GOBET, E., LEMOR, J.-P., AND WARIN, X. A regression-based Monte Carlo method to solve backward stochastic differential equations. *Ann. Appl. Probab.* 15, 3 (2005), 2172–2202.
- [90] GOBET, E., LÓPEZ-SALAS, J. G., TURKEDJIEV, P., AND VÁZQUEZ, C. Stratified regression Monte-Carlo scheme for semilinear PDEs and BSDEs with large scale parallelization on GPUs. *SIAM J. Sci. Comput.* 38, 6 (2016), C652–C677.
- [91] GOBET, E., AND TURKEDJIEV, P. Approximation of backward stochastic differential equations using Malliavin weights and least-squares regression. *Bernoulli* 22, 1 (2016), 530–562.
- [92] GOBET, E., AND TURKEDJIEV, P. Linear regression MDP scheme for discrete backward stochastic differential equations under general conditions. *Math. Comput.* 85, 299 (2016), 1359–1391.
- [93] GONON, L. Random feature neural networks learn Black–Scholes type PDEs without curse of dimensionality. *arXiv:2106.08900* (2021), 46 pages.
- [94] GONON, L., GROHS, P., JENTZEN, A., KOFLER, D., AND ŠIŠKA, D. Uniform error estimates for artificial neural network approximations for heat equations. *IMA J. Numer. Anal.* (2021), 64 pp.
- [95] GONON, L., MUHLE-KARBE, J., AND SHI, X. Asset pricing with general transaction costs: theory and numerics. *Math. Finance* 31, 2 (2021), 595–648.
- [96] GONON, L., AND SCHWAB, C. Deep ReLU network expression rates for option prices in high-dimensional, exponential Lévy models. Tech. Rep. 2020-52, Seminar for Applied Mathematics, ETH Zürich, Switzerland, 2020.
- [97] GORIKHOVSKII, V. I., EVDOKIMOVA, T. O., AND POLETANSKY, V. A. Neural networks in solving differential equations. *J. Phys. Conf. Ser.* 2308, 1 (jul 2022), 012008.
- [98] GOUDENÈGE, L., MOLENT, A., AND ZANETTE, A. Variance reduction applied to machine learning for pricing Bermudan/American options in high dimension. *arXiv:1903.11275* (2019), 25 pages.
- [99] GROHS, P., AND HERRMANN, L. Deep neural network approximation for high-dimensional elliptic PDEs with boundary conditions. *IMA J. Numer. Anal.* 42, 3 (2022), 2055–2082.
- [100] GROHS, P., HORNUNG, F., JENTZEN, A., AND VON WURSTEMBERGER, P. A proof that artificial neural networks overcome the curse of dimensionality in the numerical approximation of Black-Scholes partial differential equations. *To appear in Mem. Amer. Math. Soc., arXiv:1809.02362* (2018), 124 pages.
- [101] GROHS, P., JENTZEN, A., AND SALIMOVA, D. Deep neural network approximations for solutions of PDEs based on Monte Carlo algorithms. *Partial Differ. Equ. Appl.* 3, 4 (2022), 45, 41 pp.
- [102] GUO, L., WU, H., YU, X., AND ZHOU, T. Monte Carlo fPINNs: Deep learning method for forward and inverse problems involving high dimensional fractional partial differential equations. *Comput. Methods Appl. Mech. Engrg.* 400 (2022), 115523.
- [103] GYÖNGY, I., AND KRYLOV, N. On the splitting-up method and stochastic partial differential equations. *Ann. Probab.* 31, 2 (2003), 564–591.

- [104] GÜLER, B., LAIGNELET, A., AND PARPAS, P. Towards Robust and Stable Deep Learning Algorithms for Forward Backward Stochastic Differential Equations. *arXiv:1910.11623* (2019), 10 pages.
- [105] HAGHIGHAT, E., BEKAR, A. C., MADENCI, E., AND JUANES, R. A nonlocal physics-informed deep learning framework using the peridynamic differential operator. *Comput. Methods Appl. Mech. Engrg.* 385 (2021).
- [106] HAIRER, M., HUTZENTHALER, M., AND JENTZEN, A. Loss of regularity for Kolmogorov equations. *Ann. Probab.* 43, 2 (2015), 468–527.
- [107] HAN, J., AND HU, R. Deep fictitious play for finding Markovian Nash equilibrium in multi-agent games. In *Proceedings of The First Mathematical and Scientific Machine Learning Conference (MSML)* (2020), vol. 107, pp. 221–245.
- [108] HAN, J., HU, R., AND LONG, J. Convergence of deep fictitious play for stochastic differential games. *Front. Math. Finance* 1, 2 (2022), 287–319.
- [109] HAN, J., JENTZEN, A., AND E, W. Solving high-dimensional partial differential equations using deep learning. *Proc. Natl. Acad. Sci. USA* 115, 34 (2018), 8505–8510.
- [110] HAN, J., AND LONG, J. Convergence of the deep BSDE method for coupled FBSDEs. *Prob. Uncertain. Quant. Risk* 5, 5 (2020).
- [111] HAN, J., LU, J., AND ZHOU, M. Solving high-dimensional eigenvalue problems using deep neural networks: A diffusion Monte Carlo like approach. *J. Comput. Phys.* 423 (2020), 109792.
- [112] HAN, J., NICA, M., AND STINCHCOMBE, A. R. A derivative-free method for solving elliptic partial differential equations with deep neural networks. *J. Comput. Phys.* 419 (2020), 109672.
- [113] HAN, J., ZHANG, L., AND E, W. Solving many-electron Schrödinger equation using deep neural networks. *J. Comput. Phys.* 399 (2019), 108929.
- [114] HEINRICH, S. Monte Carlo complexity of global solution of integral equations. *J. Complex.* 14, 2 (1998), 151–175.
- [115] HEINRICH, S. Multilevel Monte Carlo methods. In *International Conference on Large-Scale Scientific Computing* (2001), Springer, pp. 58–67.
- [116] HEINRICH, S., AND SINDAMBIWE, E. Monte Carlo complexity of parametric integration. *J. Complex.* 15, 3 (1999), 317–341.
- [117] HENRY-LABORDÈRE, P. Counterparty risk valuation: A marked branching diffusion approach. *arXiv:1203.2369* (2012), 17 pages.
- [118] HENRY-LABORDÈRE, P. Deep Primal-Dual Algorithm for BSDEs: Applications of Machine Learning to CVA and IM. *Available at SSRN 3071506* (2017).
- [119] HENRY-LABORDÈRE, P., OUDJANE, N., TAN, X., TOUZI, N., AND WARIN, X. Branching diffusion representation of semilinear PDEs and Monte Carlo approximation. *Ann. Inst. Henri Poincaré Probab. Stat.* 55, 1 (2019), 184–210.
- [120] HENRY-LABORDÈRE, P., TAN, X., AND TOUZI, N. A numerical algorithm for a class of BSDEs via the branching process. *Stochastic Process. Appl.* 124, 2 (2014), 1112–1140.
- [121] HERMANN, J., SCHÄTZLE, Z., AND NOÉ, F. Deep-neural-network solution of the electronic Schrödinger equation. *Nature Chem.* 12, 10 (Oct 2020), 891–897.
- [122] HOCHBRUCK, M., AND OSTERMANN, A. Explicit exponential Runge–Kutta methods for semilinear parabolic problems. *SIAM J. Numer. Anal.* 43, 3 (2005), 1069–1090.

- [123] HORNING, F., JENTZEN, A., AND SALIMOVA, D. Space-time deep neural network approximations for high-dimensional partial differential equations. *arXiv:2006.02199* (2020), 52 pages.
- [124] HOROWITZ, M. B., DAMLE, A., AND BURDICK, J. W. Linear Hamilton Jacobi Bellman equations in high dimensions. In *53rd IEEE Conference on Decision and Control* (2014), pp. 5880–5887.
- [125] HU, Y., NUALART, D., AND SONG, X. Malliavin calculus for backward stochastic differential equations and application to numerical solutions. *Ann. Appl. Probab.* *21*, 6 (2011), 2379–2423.
- [126] HU, Z., JAGTAP, A. D., KARNIADAKIS, G. E., AND KAWAGUCHI, K. When do extended physics-informed neural networks (XPINNs) improve generalization? *SIAM J. Sci. Comput.* *44*, 5 (2022), A3158–A3182.
- [127] HURÉ, C., PHAM, H., AND WARIN, X. Deep backward schemes for high-dimensional nonlinear PDEs. *Math. Comp.* *89*, 324 (2020), 1547–1579.
- [128] HUTZENTHALER, M., JENTZEN, A., AND KRUSE, T. Overcoming the curse of dimensionality in the numerical approximation of parabolic partial differential equations with gradient-dependent nonlinearities. *Found. Comput. Math.* (2021), 62 pp.
- [129] HUTZENTHALER, M., JENTZEN, A., KRUSE, T., ANH NGUYEN, T., AND VON WURSTEMBERGER, P. Overcoming the curse of dimensionality in the numerical approximation of semilinear parabolic partial differential equations. *Proc. A.* *476*, 2244 (2020), 20190630.
- [130] HUTZENTHALER, M., JENTZEN, A., KRUSE, T., AND NGUYEN, T. A. Multilevel Picard approximations for high-dimensional semilinear second-order PDEs with Lipschitz nonlinearities. *arXiv:2009.02484* (2020), 37 pages.
- [131] HUTZENTHALER, M., JENTZEN, A., KRUSE, T., AND NGUYEN, T. A. A proof that rectified deep neural networks overcome the curse of dimensionality in the numerical approximation of semilinear heat equations. *Partial Differ. Equ. Appl.* *1* (2020), 1–34.
- [132] HUTZENTHALER, M., JENTZEN, A., AND VON WURSTEMBERGER, P. Overcoming the curse of dimensionality in the approximative pricing of financial derivatives with default risks. *Electron. J. Probab.* *25* (2020), 73 pages.
- [133] HUTZENTHALER, M., AND KRUSE, T. Multilevel Picard approximations of high-dimensional semilinear parabolic differential equations with gradient-dependent nonlinearities. *SIAM J. Numer. Anal.* *58*, 2 (2020), 929–961.
- [134] IMKELLER, P., DOS REIS, G., AND ZHANG, J. Results on numerics for FBSDE with drivers of quadratic growth. In *Contemporary Quantitative Finance*. Springer, 2010, pp. 159–182.
- [135] IOFFE, S., AND SZEGEDY, C. Batch Normalization: Accelerating deep network training by reducing internal covariate shift. *arXiv:1502.03167* (2015), 11 pages.
- [136] JACQUIER, A. J., AND OUMGARI, M. Deep curve-dependent PDEs for affine rough volatility. *arXiv:1906.02551* (2019), 20 pages.
- [137] JAGTAP, A. D., AND KARNIADAKIS, G. E. Extended physics-informed neural networks (XPINNs): A generalized space-time domain decomposition based deep learning framework for nonlinear partial differential equations. *Comm. Comput. Phys.* *28*, 5 (2020), 2002–2041.
- [138] JAGTAP, A. D., KAWAGUCHI, K., AND EM KARNIADAKIS, G. Locally adaptive activation functions with slope recovery for deep and physics-informed neural networks. *Proc. A.* *476*, 2239 (2020), 20200334.

- [139] JAGTAP, A. D., KAWAGUCHI, K., AND KARNIADAKIS, G. E. Adaptive activation functions accelerate convergence in deep and physics-informed neural networks. *J. Comput. Phys.* **404** (2020), 109136.
- [140] JAGTAP, A. D., KHARAZMI, E., AND KARNIADAKIS, G. E. Conservative physics-informed neural networks on discrete domains for conservation laws: Applications to forward and inverse problems. *Comput. Methods Appl. Mech. Engrg.* **365** (2020), 113028.
- [141] JENTZEN, A. Pathwise numerical approximation of SPDEs with additive noise under non-global Lipschitz coefficients. *Potential Anal.* **31**, 4 (2009), 375–404.
- [142] JENTZEN, A., SALIMOVA, D., AND WELTI, T. A proof that deep artificial neural networks overcome the curse of dimensionality in the numerical approximation of Kolmogorov partial differential equations with constant diffusion and nonlinear drift coefficients. *Commun. Math. Sci.* **19**, 5 (2021), 1167–1205.
- [143] JI, S., PENG, S., PENG, Y., AND ZHANG, X. Three algorithms for solving high-dimensional fully coupled FBSDEs through deep learning. *IEEE Intell. Syst.* **35**, 3 (2020), 71–84.
- [144] JIANG, Y., AND LI, J. Convergence of the deep BSDE method for FBSDEs with non-Lipschitz coefficients. *Prob. Uncertain. Quant. Risk* **6**, 4 (2021), 391.
- [145] JIANYU, L., SIWEI, L., YINGJIAN, Q., AND YAPING, H. Numerical solution of elliptic partial differential equation using radial basis function neural networks. *Neural Netw.* **16**, 5-6 (2003), 729–734.
- [146] JIN, X., CAI, S., LI, H., AND KARNIADAKIS, G. E. NSFnets (Navier-Stokes flow nets): Physics-informed neural networks for the incompressible Navier-Stokes equations. *J. Comput. Phys.* **426** (2021), 109951.
- [147] KARATZAS, I., AND SHREVE, S. *Brownian Motion and Stochastic Calculus*, 2nd ed. Springer New York, NY, 1998.
- [148] KARNIADAKIS, G. E., KEVREKIDIS, I. G., LU, L., PERDIKARIS, P., WANG, S., AND YANG, L. Physics-informed machine learning. *Nat. Rev. Phys.* **3**, 6 (Jun 2021), 422–440.
- [149] KARUMURI, S., TRIPATHY, R., BILIONIS, I., AND PANCHAL, J. Simulator-free solution of high-dimensional stochastic elliptic partial differential equations using deep neural networks. *J. Comput. Phys.* **404** (2020), 109120.
- [150] KHARAZMI, E., ZHANG, Z., AND KARNIADAKIS, G. E. Variational physics-informed neural networks for solving partial differential equations. *arXiv:1912.00873* (2019), 24 pages.
- [151] KHARAZMI, E., ZHANG, Z., AND KARNIADAKIS, G. E. hp-VPINNs: Variational physics-informed neural networks with domain decomposition. *Comput. Methods Appl. Mech. Engrg.* **374** (2021), 113547.
- [152] KHOO, Y., LU, J., AND YING, L. Solving for high-dimensional committor functions using artificial neural networks. *Res. Math. Sci.* **6**, 1 (2019).
- [153] KHOO, Y., LU, J., AND YING, L. Solving parametric PDE problems with artificial neural networks. *European J. Appl. Math.* (2020), 1–15.
- [154] KHOO, Y., AND YING, L. SwitchNet: a neural network model for forward and inverse scattering problems. *SIAM J. Sci. Comput.* **41**, 5 (2019), A3182–A3201.
- [155] KINGMA, D. P., AND BA, J. Adam: A method for stochastic optimization. *arXiv:1412.6980* (2014), 15 pages.
- [156] KISSAS, G., YANG, Y., HWUANG, E., WITSCHHEY, W. R., DETRE, J. A., AND PERDIKARIS, P. Machine learning in cardiovascular flows modeling: Predicting arterial blood pressure from non-invasive 4D flow MRI data using physics-informed neural networks. *Comput. Methods Appl. Mech. Engrg.* **358** (2020), 112623.

- [157] KREMSNER, S., STEINICKE, A., AND SZÖLGYENYI, M. A deep neural network algorithm for semilinear elliptic PDEs with applications in insurance mathematics. *Risks* 8, 4 (2020).
- [158] KRISHNAPRIYAN, A., GHOLAMI, A., ZHE, S., KIRBY, R., AND MAHONEY, M. W. Characterizing possible failure modes in physics-informed neural networks. In *Advances in Neural Information Processing Systems* (2021), M. Ranzato, A. Beygelzimer, Y. Dauphin, P. Liang, and J. W. Vaughan, Eds., vol. 34, Curran Associates, Inc., pp. 26548–26560.
- [159] KUTYNIOK, G., PETERSEN, P., RASLAN, M., AND SCHNEIDER, R. A theoretical analysis of deep neural networks and parametric PDEs. *Constr. Approx.* 55, 1 (2022), 73–125.
- [160] LABART, C., AND LELONG, J. A parallel algorithm for solving BSDEs. *Monte Carlo Methods Appl.* 19, 1 (2013), 11–39.
- [161] LAGARIS, I. E., LIKAS, A., AND FOTIADIS, D. I. Artificial neural networks for solving ordinary and partial differential equations. *IEEE Trans. Neural Netw.* 9, 5 (1998), 987–1000.
- [162] LE CAVIL, A., OUDJANE, N., AND RUSSO, F. Particle system algorithm and chaos propagation related to non-conservative McKean type stochastic differential equations. *Stoch. Partial Differ. Equ. Anal. Comput.* 5, 1 (2017), 1–37.
- [163] LE CAVIL, A., OUDJANE, N., AND RUSSO, F. Monte-Carlo algorithms for a forward Feynman–Kac-type representation for semilinear nonconservative partial differential equations. *Monte Carlo Methods Appl.* 24, 1 (2018), 55–70.
- [164] LE CAVIL, A., OUDJANE, N., AND RUSSO, F. Forward Feynman-Kac type representation for semilinear non-conservative partial differential equations. *Stochastics* 91, 8 (2019), 1206–1248.
- [165] LEMOR, J.-P., GOBET, E., AND WARIN, X. Rate of convergence of an empirical regression method for solving generalized backward stochastic differential equations. *Bernoulli* 12, 5 (2006), 889–916.
- [166] LI, J., CHEN, J., AND LI, B. Gradient-optimized physics-informed neural networks (GOPINNs): a deep learning method for solving the complex modified KdV equation. *Nonlinear Dyn.* 107, 1 (Jan 2022), 781–792.
- [167] LI, K., TANG, K., WU, T., AND LIAO, Q. D3M: A deep domain decomposition method for partial differential equations. *IEEE Access* 8 (2020), 5283–5294.
- [168] LI, Z., KOVACHKI, N., AZIZZADENESHELI, K., LIU, B., BHATTACHARYA, K., STUART, A., AND ANANDKUMAR, A. Fourier neural operator for parametric partial differential equations. *arXiv:2010.08895* (2020), 16 pages.
- [169] LIN, A. T., FUNG, S. W., LI, W., NURBEKYAN, L., AND OSHER, S. J. Alternating the population and control neural networks to solve high-dimensional stochastic mean-field games. *Proc. Natl. Acad. Sci. USA* 118, 31 (2021), e2024713118.
- [170] LONG, Z., LU, Y., AND DONG, B. PDE-Net 2.0: Learning PDEs from data with a numeric-symbolic hybrid deep network. *J. Comput. Phys.* 399 (2019), 108925.
- [171] LONG, Z., LU, Y., MA, X., AND DONG, B. PDE-Net: Learning PDEs from data. In *Proceedings of the 35th International Conference on Machine Learning* (2018), J. Dy and A. Krause, Eds., vol. 80, PMLR, pp. 3208–3216.
- [172] LONGO, M., MISHRA, S., RUSCH, T. K., AND SCHWAB, C. Higher-order quasi-Monte Carlo training of deep neural networks. *SIAM J. Sci. Comput.* 43, 6 (2021), A3938–A3966.
- [173] LU, L., MENG, X., MAO, Z., AND KARNIADAKIS, G. E. DeepXDE: a deep learning library for solving differential equations. *SIAM Rev.* 63, 1 (2021), 208–228.

- [174] LUO, D., AND CLARK, B. K. Backflow transformations via neural networks for quantum many-body wave functions. *Phys. Rev. Lett.* 122, 22 (2019), 226401.
- [175] LUO, T., AND YANG, H. Two-Layer Neural Networks for Partial Differential Equations: Optimization and Generalization Theory. *arXiv:2006.15733* (2020), 30 pages.
- [176] LYE, K. O., MISHRA, S., AND RAY, D. Deep learning observables in computational fluid dynamics. *J. Comput. Phys.* (2020), 109339.
- [177] LYE, K. O., MISHRA, S., RAY, D., AND CHANDRASHEKAR, P. Iterative surrogate model optimization (ISMO): an active learning algorithm for PDE constrained optimization with deep neural networks. *Comput. Methods Appl. Mech. Engrg.* 374 (2021), Paper No. 113575, 27.
- [178] MA, J., PROTTER, P., SAN MARTÍN, J., AND TORRES, S. Numerical method for backward stochastic differential equations. *Ann. Appl. Probab.* 12, 1 (2002), 302–316.
- [179] MAGILL, M., QURESHI, F., AND DE HAAN, H. Neural networks trained to solve differential equations learn general representations. In *Advances in Neural Information Processing Systems* (2018), pp. 4071–4081.
- [180] MAO, Z., JAGTAP, A. D., AND KARNIADAKIS, G. E. Physics-informed neural networks for high-speed flows. *Comput. Methods Appl. Mech. Engrg.* 360 (2020), 112789.
- [181] MARTINEZ, M., SAN MARTÍN, J., AND TORRES, S. Numerical method for reflected backward stochastic differential equations. *Stoch. Anal. Appl.* 29, 6 (2011), 1008–1032.
- [182] MCCLENNY, L., AND BRAGA-NETO, U. Self-adaptive physics-informed neural networks using a soft attention mechanism. *arXiv:2009.04544* (2020).
- [183] MENG, X., LI, Z., ZHANG, D., AND KARNIADAKIS, G. E. PPINN: Parareal physics-informed neural network for time-dependent PDEs. *Comput. Methods Appl. Mech. Engrg.* 370 (2020).
- [184] MICHOSKI, C., MILOSAVLJEVIĆ, M., OLIVER, T., AND HATCH, D. R. Solving differential equations using deep neural networks. *Neurocomputing* 399 (2020), 193–212.
- [185] MISHRA, S., AND MOLINARO, R. Estimates on the generalization error of physics-informed neural networks for approximating a class of inverse problems for PDEs. *IMA J. Numer. Anal.* 42, 2 (06 2021), 981–1022.
- [186] MISHRA, S., AND MOLINARO, R. Physics informed neural networks for simulating radiative transfer. *J. Quant. Spectrosc. Radiat. Transf.* 270 (2021), 107705.
- [187] MISRA, D. Mish: A self regularized non-monotonic activation function. *arXiv:1908.08681* (2019), 14 pages.
- [188] MÜLLER, J., AND ZEINHOFFER, M. Deep Ritz revisited. *arXiv:1912.03937* (2019), 10 pages.
- [189] NABIAN, M. A., AND MEIDANI, H. A deep learning solution approach for high-dimensional random differential equations. *Probab. Engrg. Mech.* 57 (2019), 14–25.
- [190] NAKAMURA-ZIMMERER, T., GONG, Q., AND KANG, W. A causality-free neural network method for high-dimensional Hamilton–Jacobi–Bellman equations. In *2020 American Control Conference (ACC)* (2020), pp. 787–793.
- [191] NÜSKEN, N., AND RICHTER, L. Solving high-dimensional Hamilton–Jacobi–Bellman PDEs using neural networks: perspectives from the theory of controlled diffusions and measures on path space. *Partial Differ. Equ. Appl.* 2, 4 (Jun 2021), 48.
- [192] ØKSENDAL, B. *Stochastic Differential Equations: An Introduction with Applications*, 5th ed. Springer Berlin Heidelberg, 1998.

- [193] PANG, G., D’ELIA, M., PARKS, M., AND KARNIADAKIS, G. nPINNs: Nonlocal physics-informed neural networks for a parametrized nonlocal universal Laplacian operator. Algorithms and applications. *J. Comput. Phys.* 422 (2020), 109760.
- [194] PANG, G., LU, L., AND KARNIADAKIS, G. E. fPINNs: Fractional physics-informed neural networks. *SIAM J. Sci. Comput.* 41, 4 (2019), A2603–A2626.
- [195] PARDOUX, E., AND PENG, S. Backward stochastic differential equations and quasilinear parabolic partial differential equations. In *Stochastic partial differential equations and their applications (Charlotte, NC, 1991)*, vol. 176 of *Lect. Notes Control Inf. Sci.* Springer, Berlin, 1992, pp. 200–217.
- [196] PARDOUX, E., AND PENG, S. G. Adapted solution of a backward stochastic differential equation. *Systems Control Lett.* 14, 1 (1990), 55–61.
- [197] PENG, S. G. Probabilistic interpretation for systems of quasilinear parabolic partial differential equations. *Stochastics Stochastics Rep.* 37, 1-2 (1991), 61–74.
- [198] PEREIRA, M. A., WANG, Z., CHEN, T., REED, E., AND THEODOROU, E. Feynman–Kac Neural Network Architectures for Stochastic Control Using Second-Order FBSDE Theory. In *Proceedings of the 2nd Conference on Learning for Dynamics and Control* (2020), vol. 120, PMLR, pp. 728–738.
- [199] PEREIRA, M. A., WANG, Z., EXARCHOS, I., AND THEODOROU, E. A. Learning Deep Stochastic Optimal Control Policies Using Forward-Backward SDEs. In *Robotics: Science and Systems* (2019).
- [200] PESKIR, G., AND SHIRYAEV, A. *Optimal stopping and free-boundary problems*. Lectures in Mathematics ETH Zürich. Birkhäuser Verlag, Basel, 2006.
- [201] PFAU, D., SPENCER, J. S., MATTHEWS, A. G. D. G., AND FOULKES, W. M. C. Ab initio solution of the many-electron Schrödinger equation with deep neural networks. *Phys. Rev. Research* 2 (2020), 033429.
- [202] PHAM, H., WARIN, X., AND GERMAIN, M. Neural networks-based backward scheme for fully nonlinear PDEs. *Partial Differ. Equ. Appl.* 2, 1 (2021), Paper No. 16, 24.
- [203] RAISSI, M. Deep hidden physics models: Deep learning of nonlinear partial differential equations. *J. Mach. Learn. Res.* 19, 1 (2018), 932–955.
- [204] RAISSI, M. Forward-backward stochastic neural networks: Deep learning of high-dimensional partial differential equations. *arXiv:1804.07010* (2018), 17 pages.
- [205] RAISSI, M., PERDIKARIS, P., AND KARNIADAKIS, G. E. Physics Informed Deep Learning (Part I): Data-driven Solutions of Nonlinear Partial Differential Equations. *arXiv:1711.10561* (2017), 22 pages.
- [206] RAISSI, M., PERDIKARIS, P., AND KARNIADAKIS, G. E. Physics Informed Deep Learning (Part II): Data-driven Discovery of Nonlinear Partial Differential Equations. *arXiv:1711.10566* (2017), 19 pages.
- [207] RAISSI, M., PERDIKARIS, P., AND KARNIADAKIS, G. E. Numerical Gaussian processes for time-dependent and nonlinear partial differential equations. *SIAM J. Sci. Comput.* 40, 1 (2018), A172–A198.
- [208] RAISSI, M., PERDIKARIS, P., AND KARNIADAKIS, G. E. Physics-informed neural networks: A deep learning framework for solving forward and inverse problems involving nonlinear partial differential equations. *J. Comput. Phys.* 378 (2019), 686–707.
- [209] REISINGER, C., AND ZHANG, Y. Rectified deep neural networks overcome the curse of dimensionality for nonsmooth value functions in zero-sum games of nonlinear stiff systems. *Anal. Appl. (Singap.)* 18, 6 (2020), 951–999.

- [210] RICHOU, A. Numerical simulation of BSDEs with drivers of quadratic growth. *Ann. Appl. Probab.* 21, 5 (2011), 1933–1964.
- [211] RICHOU, A. Markovian quadratic and superquadratic BSDEs with an unbounded terminal condition. *Stochastic Process. Appl.* 122, 9 (2012), 3173–3208.
- [212] RICHTER, L., SALLANDT, L., AND NÜSKEN, N. Solving high-dimensional parabolic PDEs using the tensor train format. In *Proceedings of the 38th International Conference on Machine Learning* (18–24 Jul 2021), M. Meila and T. Zhang, Eds., vol. 139 of *Proceedings of Machine Learning Research*, PMLR, pp. 8998–9009.
- [213] RUIJTER, M. J., AND OOSTERLEE, C. W. A Fourier cosine method for an efficient computation of solutions to BSDEs. *SIAM J. Sci. Comput.* 37, 2 (2015), A859–A889.
- [214] RUIJTER, M. J., AND OOSTERLEE, C. W. Numerical Fourier method and second-order Taylor scheme for backward SDEs in finance. *Appl. Numer. Math.* 103 (2016), 1–26.
- [215] RUTHOTTO, L., OSHER, S. J., LI, W., NURBEKYAN, L., AND FUNG, S. W. A machine learning framework for solving high-dimensional mean field game and mean field control problems. *Proc. Natl. Acad. Sci. USA* 117, 17 (2020), 9183–9193.
- [216] SABATE VIDALES, M., ŠIŠKA, D., AND SZPRUCH, L. Unbiased deep solvers for linear parametric PDEs. *Appl. Math. Finance* 28, 4 (2021), 299–329.
- [217] SAMANIEGO, E., ANITESCU, C., GOSWAMI, S., NGUYEN-THANH, V., GUO, H., HAMDIA, K., ZHUANG, X., AND RABCZUK, T. An energy approach to the solution of partial differential equations in computational mechanics via machine learning: Concepts, implementation and applications. *Comput. Methods Appl. Mech. Engrg.* 362 (2020), 112790.
- [218] SHENG, H., AND YANG, C. PFNN: A penalty-free neural network method for solving a class of second-order boundary-value problems on complex geometries. *J. Comput. Phys.* 428 (2021), 110085.
- [219] SHIN, Y., DARBON, J., AND KARNIADAKIS, G. E. On the convergence of physics informed neural networks for linear second-order elliptic and parabolic type PDEs. *Comm. Comput. Phys.* 28, 5 (2020), 2042–2074.
- [220] SIRIGNANO, J., AND SPILIOPOULOS, K. DGM: A deep learning algorithm for solving partial differential equations. *J. Comput. Phys.* 375 (2018), 1339–1364.
- [221] SKOROKHOD, A. V. Branching diffusion processes. *Theory Probab. Its Appl.* 9, 3 (1964), 445–449.
- [222] TENG, L., LAPITCKII, A., AND GÜNTHER, M. A multi-step scheme based on cubic spline for solving backward stochastic differential equations. *Appl. Numer. Math.* 150 (2020), 117–138.
- [223] UCHIYAMA, T., AND SONEHARA, N. Solving inverse problems in nonlinear PDEs by recurrent neural networks. In *IEEE International Conference on Neural Networks* (1993), IEEE, pp. 99–102.
- [224] VAN MOERBEKE, P. On optimal stopping and free boundary problems. *Arch. Rational Mech. Anal.* 60 (1976), 101–148.
- [225] WANG, S., AND PERDIKARIS, P. Deep learning of free boundary and Stefan problems. *J. Comput. Phys.* (2020), 109914.
- [226] WANG, S., TENG, Y., AND PERDIKARIS, P. Understanding and mitigating gradient flow pathologies in physics-informed neural networks. *SIAM J. Sci. Comput.* 43, 5 (2021), A3055–A3081.

- [227] WANG, S., WANG, H., AND PERDIKARIS, P. On the eigenvector bias of Fourier feature networks: From regression to solving multi-scale PDEs with physics-informed neural networks. *Comput. Methods Appl. Mech. Engrg.* 384 (2021), 113938.
- [228] WANG, Z., AND ZHANG, Z. A mesh-free method for interface problems using the deep learning approach. *J. Comput. Phys.* 400 (2020), 108963.
- [229] WARIN, X. Variations on branching methods for non linear PDEs. *arXiv:1701.07660* (2017), 25 pages.
- [230] WARIN, X. Monte Carlo for high-dimensional degenerated semi linear and full non linear PDEs. *arXiv:1805.05078* (2018), 23 pages.
- [231] WARIN, X. Nesting Monte Carlo for high-dimensional non-linear PDEs. *SIAM J. Numer. Anal.* 24, 4 (2018), 225–247.
- [232] WATANABE, S. On the branching process for Brownian particles with an absorbing boundary. *J. Math. Kyoto Univ.* 4, 2 (1965), 385–398.
- [233] WIGHT, C. L., AND ZHAO, J. Solving Allen-Cahn and Cahn-Hilliard equations using the adaptive physics informed neural networks. *Comm. Comput. Phys.* 29, 3 (2021), 930–954.
- [234] XU, H., CHEN, J., AND MA, F. Adaptive deep learning approximation for Allen-Cahn equation. In *Computational Science – ICCS 2022: 22nd International Conference, London, UK, June 21–23, 2022, Proceedings, Part IV* (Berlin, Heidelberg, 2022), Springer-Verlag, p. 271–283.
- [235] YANG, L., ZHANG, D., AND KARNIADAKIS, G. E. Physics-informed generative adversarial networks for stochastic differential equations. *SIAM J. Sci. Comput.* 42, 1 (2020), A292–A317.
- [236] YU, J., LU, L., MENG, X., AND KARNIADAKIS, G. E. Gradient-enhanced physics-informed neural networks for forward and inverse PDE problems. *Comput. Methods Appl. Mech. Engrg.* 393 (2022), 114823.
- [237] YUAN, L., NI, Y.-Q., DENG, X.-Y., AND HAO, S. A-PINN: Auxiliary physics informed neural networks for forward and inverse problems of nonlinear integro-differential equations. *J. Comput. Phys.* (2022), Article No. 111260. Early access version available online.
- [238] ZANG, Y., BAO, G., YE, X., AND ZHOU, H. Weak adversarial networks for high-dimensional partial differential equations. *J. Comput. Phys.* 411 (2020), 109409.
- [239] ZHANG, D., GUO, L., AND KARNIADAKIS, G. E. Learning in modal space: Solving time-dependent stochastic PDEs using physics-informed neural networks. *SIAM J. Sci. Comput.* 42, 2 (2020), A639–A665.
- [240] ZHANG, D., LU, L., GUO, L., AND KARNIADAKIS, G. E. Quantifying total uncertainty in physics-informed neural networks for solving forward and inverse stochastic problems. *J. Comput. Phys.* 397 (2019), 108850.
- [241] ZHAO, W., FU, Y., AND ZHOU, T. New kinds of high-order multistep schemes for coupled forward backward stochastic differential equations. *SIAM J. Sci. Comput.* 36, 4 (2014), A1731–A1751.
- [242] ZHAO, W., ZHANG, G., AND JU, L. A stable multistep scheme for solving backward stochastic differential equations. *SIAM J. Numer. Anal.* 48, 4 (2010), 1369–1394.
- [243] ZHU, Y., ZABARAS, N., KOUTSOURELAKIS, P.-S., AND PERDIKARIS, P. Physics-constrained deep learning for high-dimensional surrogate modeling and uncertainty quantification without labeled data. *J. Comput. Phys.* 394 (2019), 56–81.

- [244] ZUBOV, K., MCCARTHY, Z., MA, Y., CALISTO, F., PAGLIARINO, V., AZEGLIO, S., BOTTERO, L., LUJÁN, E., SULZER, V., BHARAMBE, A., VINCHHI, N., BALAKRISHNAN, K., UPADHYAY, D., AND RACKAUCKAS, C. NeuralPDE: Automating Physics-Informed Neural Networks (PINNs) with Error Approximations. *arXiv:2107.09443* (2021), 77 pages.